Journal of
Mechanics of
Materials and Structures

SIZE-NORMALIZED ROBUSTNESS OF Dpp GRADIENT IN *DROSOPHILA* WING IMAGINAL DISC

Arthur D. Lander, Qing Nie, Benjamin Vargas and Frederic Y. M. Wan

Volume 6, No. 1-4 January–June 2011

mathematical sciences publishers

JOURNAL OF MECHANICS OF MATERIALS AND STRUCTURES
Vol. 6, No. 1-4, 2011

SIZE-NORMALIZED ROBUSTNESS OF Dpp GRADIENT IN *DROSOPHILA* WING IMAGINAL DISC

ARTHUR D. LANDER, QING NIE, BENJAMIN VARGAS AND FREDERIC Y. M. WAN

Dedicated to Charles and Marie-Louise Steele for their years of outstanding management of IJSS and JoMMS, and for their more than forty years of warm friendship with the last author.

Exogenous environmental changes are known to affect the intrinsic characteristics of biological organisms. For instance, the synthesis rate of the morphogen decapentaplegic (Dpp) in a *Drosophila* wing imaginal disc has been found to double with an increase of 5.9°C in ambient temperature. If not compensated, such a change would alter the signaling Dpp gradient significantly and thereby the development of the wing imaginal disc. To learn how flies continue to develop "normally" under such an exogenous change, we formulate in this paper a spatially two-dimensional reaction-diffusion system of partial differential equations (PDE) that accounts for the biological processes at work in the *Drosophila* wing disc essential for the formation of signaling Dpp gradient. By way of this PDE model, we investigate the effect of the apical-basal thickness and anteroposterior span of the wing on the shape of signaling gradients and the robustness of wing development in an altered environment (including an enhanced morphogen synthesis rate). Our principal result is a delineation of the role of wing disc size change in maintaining the magnitude and shape of the signaling Dpp gradient. The result provides a theoretical basis for the observed robustness of wing development, preserving relative but not absolute tissue pattern, when the morphogen synthesis rate is significantly altered. A similar robustness consideration for simultaneous changes of multiple intrinsic system characteristics is also discussed briefly.

1. Morphogen gradients and temperature change

Morphogens (also known as *ligands* in biochemistry and developmental biology) are molecular substances that bind to cell surface receptors and other molecules. The concentration gradients of different morphogen-receptor complexes [Entchev et al. 2000; Gurdon and Bourillot 2001; Teleman and Cohen 2000] are known to be responsible for cell differentiation and patterning of biological tissues during the developmental phase of a biological organism. For a number of morphogen families, including Dpp in the wing imaginal disc of fruit flies of the genus *Drosophila*, it is well established experimentally and by analyses of appropriate mathematical models that the signaling gradients are formed by morphogens being transported from a localized source and binding to cell surface receptors downstream (see references cited in [Lander et al. 2002; 2005a; 2005b]). However, biochemical processes leading to morphogen gradient formation are influenced by highly cooperative events such as protein folding and membrane fluidity, and

The research was supported in part by NIH grants P50-GM076516, R01-GM067247 and R01-GM075309. The two NIH R01 grants were awarded through the Joint NSF/NIGMS Initiative to Support Research in the Area of Mathematical Biology.
Keywords: morphogen gradients, robust development, environmental changes, Dpp.

exhibit considerable idiosyncratic effects from exogenous (external environmental) changes. More specifically, it has been observed that the wing size of an adult *Drosophila* may differ by about 15% for substantially different ambient temperature, with larger fly parts in a colder climate and smaller near the equator [de Moed et al. 1997; French et al. 1998; Bitner-Mathé and Klaczko 1999; Azevedo et al. 2002]. However, similar data on *Drosophila* wing imaginal discs relevant to our investigation do not seem to be available. (An *imaginal disc* is a group of undifferentiated cells that develops, at the (later) pupa stage, into a specific adult structure such as eyes, antennae, limbs and wings, with the developmental fate of cells in different zones of such a disc determined by a different combination of morphogen gradients.) At the molecular level, we expect correspondingly that rate constants for diffusion, protein synthesis, binding, internalization, degradation, etc., of fruit flies to change in varying degrees in response to such a temperature change. How significant would such rate constant changes be over the temperature ranges organisms encounter in the wild? Surprisingly little data on this subject (at least for insect cells) can be found in the literature. Preliminary results by metabolic labeling of *Drosophila* S2 cells (through the efforts in A. D. Lander's lab, particularly by his student S. Zhou) showed that overall protein synthesis rate doubles approximately every 5.9°C. In the absence of analogous data on biochemical processes other than protein synthesis rate, we cannot explicitly explore the effects of temperature on any of the known morphogen gradient systems.

The necessity to accommodate temperature (or any other exogenous environmental) change is a major performance objective of morphogen systems. A thorough quantitative analysis of the effects of such a change on the signaling morphogen gradients is imperative. It is therefore important to be clear the reasons why we do not (and cannot) undertake such an endeavor at this time. These include:

- Experimental and field study data are available for adult *Drosophila* while the impact of ambient changes (including signaling morphogen gradient formation) starts at the embryonic stage.
- An ambient change typically affects many systems characteristics including the various rate constants and synthesis rates) but there is a lack of data on most such effects.

Still, we may obtain some insights from exact or approximate analytical solutions, qualitative analyses, and numerical simulations of mathematical models for these systems. For example, we have recently looked at effects of perturbations in which every protein synthesis rate, every endo- and exocytotic rate constant, and every degradation rate constant is doubled, but diffusion and binding constants remain unchanged [Lander et al. 2005c]. We consider such changes to constitute a crude model of the effects due to a 5.9°C temperature increase, and define robustness measures to quantify the sensitivity of the system to the changes made.

In contrast to the work in [Lander et al. 2005c] and in [Khong and Wan 2007] on the effect of a Hill-type feedback (in Dpp synthesis rate) on the signaling Dpp gradient, we pursue a different and more limited objective prompted by the observations in the works cited at the top of the page. Specifically, we determine (by analyzing appropriate mathematical models) whether and how adjusting the size of the *wing disc* (an abbreviation for "*wing imaginal disc*" henceforth) would maintain the morphogen gradient shape and thereby provide optimal, or near-optimal, strategies for meeting the performance objective of ensuring a normal development. For this more limited goal, we take as our starting point the available experimental evidence (from the Lander lab) that the Dpp synthesis rate doubles with a 5.9°C temperature increase. With all other system characteristics fixed, a change in synthesis rate would cause a change in the steady state signaling morphogen gradient, possibly substantial and unacceptable from the view

point of normal development as quantified herein (see Section 8 and also [Lander et al. 2005c]). We determine whether a particular aspect of system architecture, namely the size of wing disc, confers the potential for the biological development to be robust to such change. More specifically, the principal aim of our research is to understand

- the reason for the exaggerated slenderness of the wing disc cells in the apical-basal direction, and
- the role of a size change of the wing disc in its development.

In the process, how the signaling Dpp gradient may be maintained in the face of significant Dpp synthesis rate changes (due to a temperature or any other exogenous environmental change) is delineated.

An interesting, but challenging aspect of robustness of biological development comes from the known interrelationships between temperature, growth, and morphogen signaling. At colder temperature, flies grow slower but end up larger, including having larger but otherwise normal wings; in contrast flies grow faster and are smaller in a hotter climate [de Moed et al. 1997; French et al. 1998; Bitner-Mathé and Klaczko 1999; Azevedo et al. 2002]. The remarkably normal patterning that they display [Bitner-Mathé and Klaczko 1999] is only normal in the context of their altered size. This strongly suggests that the objective of development is to preserve relative, not absolute, pattern. At the very least we need to examine our models to see if they would allow for temperature-dependent scaling of field sizes and *size-normalized* measures of robustness.

The effect of size on the robustness of biological species development has been investigated recently — see [Umulis et al. 2008] and references therein — for general models in the form of partial differential equations of the reaction diffusion type with Neumann or mixed conditions at the boundary of the solution domain. Their main concern is uncovering conditions on the biological system characteristics that would ensure the corresponding model problem to be *scale-invariant*. Within a scale-invariant species, a common structure in individuals of different size develops in proportion to size. (We will refer to such size-mediated developments of a common biological structure as *relative (or size-mediated) robustness* as the development of structural proportion is insensitivity to size changes.) Our concern here is with a specific model of the *Drosophila* wing imaginal disc in the plane of the proximal-distal and apical-basal axes which is *not* scale-invariant and does *not* satisfy the conditions for scale-invariance developed in [Umulis et al. 2008]. Nevertheless, we show how size changes may still be exploited for such a system to maintain *near* relative robustness for size-normalized development in the presence of a significant change in its system characteristics caused by environmental perturbations. Specific quantitative measures of (relative) robustness are adopted for determining (different levels of) robustness. We investigate at first only a change in the Dpp synthesis rate for which we have experimental data, and then also simultaneous changes in several system parameters including degradation and binding rate constants for multifactor robustness. The results are consistent with the observations of smaller *Drosophila melanogaster* flies near the earth's equator and larger one in colder climates away from the equator.

Still, we may obtain some insights from exact or approximate analytical solutions, qualitative analyses, and numerical simulations of mathematical models for these systems. As mentioned earlier, we have recently looked at effects of perturbations in which every protein synthesis rate, every endo- and exocytotic rate constant, and every degradation rate constant is doubled, but diffusion and binding constants remain unchanged [Lander et al. 2005c]. We consider such changes to constitute a crude model of the effects due to a 5.9°C temperature increase, and define robustness measures to quantify the sensitivity of the system to the changes made.

2. A spatially two-dimensional formulation

We take advantage of the approximate symmetry between the anterior compartment and posterior compartment of the *Drosophila* wing imaginal disc and consider here an extracellular model of the posterior compartment. With the Dpp synthesis rate taken to be uniform in the distal-proximal direction, the development is essentially uniform along the distal-proximal axis (Y-axis) except possibly for layer phenomena near the edges (see [Vargas 2007]). Our model of the Dpp gradient formation focuses on the uniform development. This allows us to consider a typical cross section of the wing imaginal disc as in Figure 1 idealized as a rectangle orthogonal to the Y-axis away from the distal and proximal ends. We take for this rectangle X-and Z-axis to be in the anteroposterior direction and the apical-proximal direction, respectively.

The new model is essentially an extended version of the one-dimensional model in [Lander et al. 2005b] to allow for variations in the apical-basal direction including biologically realistic Dpp leakage through the basement membrane. In this new two-dimensional model, morphogen is introduced into the extracellular space at a rate V_L through a localized source uniform in the plane perpendicular to the anteroposterior direction. The localized source spans a small interval $(-X_{\min}, 0)$, where $-X_{\min}$ is the

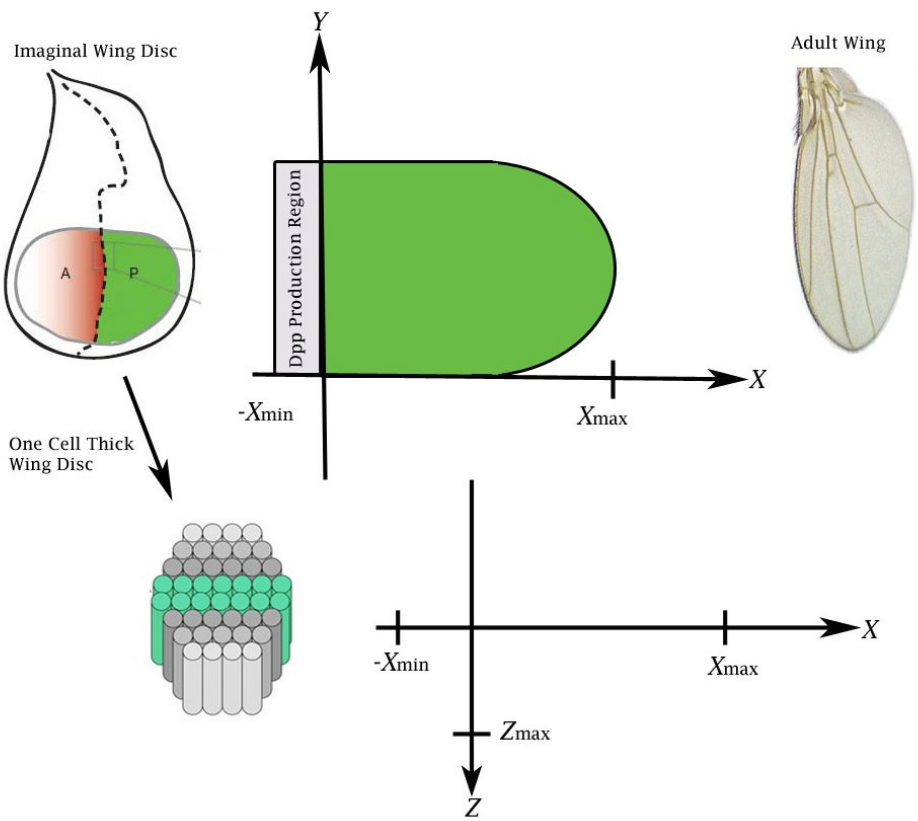

Figure 1. Wing imaginal disc and posterior compartment of *Drosophila*. Courtesy Dr. Oana Marcu of NASA Ames.

location of the border between (and the line of symmetry of) the *anterior* compartment and the *posterior* compartment of the wing disc. The morphogen produced in this localized region diffuses throughout the extracellular space in the posterior compartment (according to Fick's second law), between $Z = 0$ and $Z = Z_{\max}$ in the apical-basal direction and from $X = -X_{\min}$ toward the *sink* at the edge $X = X_{\max}$ of the posterior compartment. Along the way, some morphogen molecules bind themselves with cell surface bound receptors at the binding rate $k_{\text{on}}[L][R]$, where $[L(X, Z, T)]$ and $[R(X, Z, T)]$ are, respectively, concentration of free Dpp and unoccupied signaling receptor Thickvein (Tkv) at time T and location (X, Z). The resulting morphogen-receptor complexes of concentration $[LR(X, Z, T)]$ are bound to cell surface membrane since the receptors are. These complexes in turn *dissociate* at the rate $k_{\text{off}}[LR]$ and degrade at the rate $k_{\text{deg}}[LR]$.

The time evolution of concentrations of free morphogen, morphogen-receptor complexes and unoccupied receptors is then described by the partial differential equations (1)–(3) below governing the rate of change of $[L]$, $[LR]$ and $[R]$, respectively, with k_{on}, k_{off}, and k_{deg} known as the binding rate constant, the dissociation rate constant, and the degradation rate constant, respectively. Altogether, the three (time) rate of changes in (1)–(3) account for the reversible binding, degradation (of both bound and unoccupied receptors), and synthesis of new morphogen and receptors, analogous to the one-dimensional system of [Lou et al. 2004; Lander et al. 2005b]:

$$\frac{\partial[L]}{\partial T} = D\left(\frac{\partial^2[L]}{\partial X^2} + \frac{\partial^2[L]}{\partial Z^2}\right) - k_{\text{on}}[L][R] + k_{\text{off}}[LR] + V_L(X, Z, T), \tag{1}$$

$$\frac{\partial[LR]}{\partial T} = k_{\text{on}}[L][R] - (k_{\text{off}} + k_{\text{deg}})[LR], \tag{2}$$

$$\frac{\partial[R]}{\partial T} = V_R(X, Z, T) - k_{\text{on}}[L][R] + k_{\text{off}}[LR] - k_R[R], \tag{3}$$

for $-X_{\min} < X < X_{\max}$, $0 < Z < Z_{\max}$, and $T > 0$, where $V_L(X, Z, T)$ and $V_R(X, Z, T)$ are the rate at which the morphogen Dpp and receptors Tkv are synthesized, respectively, and k_R is the degradation rate constant for unoccupied Tkv. As in [Lander et al. 2005b], we are interested principally in the $[LR]$ gradient in the portion of the wing disc corresponding to $X > 0$ where there is no morphogen production (so that $V_L(X, Z, T) = 0$ for $X > 0$). In this paper, we focus on a time-invariant morphogen and receptor synthesis rates so that $V_L(X, Z, T) = V_L(X, Z)$ and $V_R(X, Z, T) = V_R(X, Z)$.

With $-X_{\min}$ being the midpoint of the Dpp production region, we have by symmetry

$$\text{at } X = -X_{\min}: \qquad \frac{\partial[L]}{\partial X} = 0, \tag{4}$$

for $T > 0$ and $0 < Z < Z_{\max}$. At the far end, the edge of the posterior compartment is taken to be a sink, so that

$$\text{at } X = X_{\max}: \qquad [L] = 0 \tag{5}$$

for $T > 0$ and $0 < Z < Z_{\max}$. We also investigate the limiting case of $X_{\max} = \infty$ since the edge at $X_{\max}$ is not strictly absorbing. In the apical-basal direction, we have an essentially sealed wall at the apical face $Z = 0$, so that

$$\text{at } Z = 0: \qquad \frac{\partial[L]}{\partial Z} = 0, \tag{6}$$

for $T > 0$ and $-X_{\min} < X < X_{\max}$,while at the basal face, there is leakage of free morphogens at a rate proportional to its concentration:

$$\text{at } Z = Z_{\max}: \qquad \frac{\partial [L]}{\partial Z} + \frac{\gamma_z}{Z_{\max}}[L] = 0, \tag{7}$$

for $T > 0$ and $-X_{\min} < X < X_{\max}$. Here, the dimensionless constant $\gamma_z \equiv 1/\sigma_z = Z_{\max}\Gamma_z$ is a prescribed leakage parameter. In one extreme case $\gamma_z = 0$, we have $\partial[L]/\partial Z = 0$ so that the end is sealed without leakage. At the other extreme $\sigma_z = 0$, the end $Z = Z_{\max}$ is absorbing. For a finite nonzero γ_z, the larger the γ_z value the higher is the flux across the end surface.

At the onset of the morphogen synthesis (at $T = 0$), we have the initial conditions

$$[L] = [LR] = 0, \qquad [R] = R_0(X, Z) \tag{8}$$

for $-X_{\min} \le X \le X_{\max}$ and $0 \le Z \le Z_{\max}$, reflecting the fact that there was no Dpp in the system and the receptor concentration is in a steady state (as a consequence of a time-invariant receptor synthesis rate).

The extracellular model above is adequate for our purpose. The model can be extended to incorporate the effects of internalization of $[LR]$ complexes through endocytosis prior to degradation as was done in [Lander et al. 2006; Lou et al. 2004] for one-dimensional studies. However, the corresponding system for steady state gradients of interest here has been shown to reduce to the same BVP with modified system rate constants (*loc. cit.*).

To reduce the number of parameters in the problem, we introduce a reference unoccupied receptor concentration level $\bar{R}_0$ (to be specified later) and the normalized quantities

$$t = \frac{D}{Z_{\max}^2}T, \qquad \{x, \ell_M, x_m, z\} = \frac{1}{Z_{\max}}\{X, X_{\max}, X_{\min}, Z\}, \tag{9}$$

$$\{v_L, v_R\} = \frac{Z_{\max}^2}{D\bar{R}_0}\{V_L, V_R\}, \qquad \{a, b, r, r_0\} = \frac{1}{\bar{R}_0}\{[L], [LR], [R], R_0\}, \tag{10}$$

$$\{f_z, g_z, g_r, h_z\} = \frac{1}{D/Z_{\max}^2}\{k_{\text{off}}, k_{\text{deg}}, k_R, k_{\text{on}}\bar{R}_0\}. \tag{11}$$

In terms of these new quantities, we write the initial-boundary value problem (IBVP) (1)–(8) in the normalized form

$$\frac{\partial a}{\partial t} = \nabla^2 a - h_z a r + f_z b + v_L(x, z) \qquad (x, z) \in \Omega, \tag{12}$$

$$\frac{\partial b}{\partial t} = h_z a r - (f_z + g_z)b, \qquad \frac{\partial r}{\partial t} = v_R(x, z) - h_z a r - g_r r + f_z b, \qquad (x, z) \in \bar{\Omega}, \tag{13}$$

where Ω is the rectangular domain $\{-x_m < x < \ell_M, 0 < z < 1\}$ and $\bar{\Omega} = \{-x_m \le x \le \ell_M, 0 \le z \le 1\}$ is its closure. The auxiliary conditions supplementing the differential equations become

$$\text{at } x = -x_m: \quad \frac{\partial a}{\partial x} = 0 \qquad \text{at } x = \ell_M: \quad a = 0 \qquad (0 < z < 1), \tag{14}$$

$$\text{at } z = 0: \quad \frac{\partial a}{\partial z} = 0 \qquad \text{at } z = 1: \quad \frac{\partial a}{\partial z} + \gamma_z a = 0 \qquad (-x_m < x < \ell_M), \tag{15}$$

for $t > 0$ and

$$\text{at } t = 0: \qquad a = b = 0, \qquad r = r_0(x, z) \tag{16}$$

for all (x, z) in $\bar{\Omega}$.

3. Time-independent steady state behavior

3.1. ***Time-independent synthesis rates.*** With both morphogen and the receptor synthesis rates uniform in time, the possibility of a time-independent steady state behavior exists for our model. The two synthesis rates V_L and V_R are to a good approximation uniform in Z so that $V_L = V_L(X)$ and $V_R = V_R(X)$. For the present investigation, we ignore possible feedback effects and, unless indicated otherwise, approximate V_L to be a step function with $V_L(X) = \bar{V}_L H(-X)$ for some constant $\bar{V}_L$. Correspondingly, we have with

$$v_L = v_L(x) = \bar{v}_z H(-x) = \begin{cases} \bar{v}_z \\ 0 \end{cases} \qquad \text{with } \bar{v}_z = \frac{\bar{V}_L/\bar{R}_0}{D/Z_{\max}^2}. \tag{17}$$

We also take the nonnegative receptor synthesis rate to be

$$V_R = \bar{V}_n H(-X) + \bar{V}_p H(X) = \bar{V}_p \{\rho^2 H(-X) + H(X)\},$$

for $T > 0$ with $0 \le \rho^2 = \bar{V}_n/\bar{V}_p \le 1$, unless indicated otherwise. In that case, we have

$$v_R = v_R(x) = \bar{v}_p \{\rho^2 H(-X) + H(X)\} \equiv \bar{v}_p r_0(x) \qquad (t > 0). \tag{18}$$

where

$$\bar{v}_p = \frac{\bar{V}_p/\bar{R}_0}{D/Z_{\max}^2}, \qquad r_0(x) = \begin{cases} \rho^2 & (x < 0), \\ 1 & (x > 0). \end{cases} \tag{19}$$

In the extreme case $\rho^2 = 0$, there is no receptor synthesized in the morphogen production region. At the other extreme, $\rho^2 = 1$, the receptor synthesis rate is uniform through out the posterior compartment, i.e., for all (x, z) in $\bar{\Omega}$. With the initial receptor concentration taken to be the steady state receptor distribution prior to the onset of morphogen production, $R_0(x) = V_R(X)/k_R = \bar{V}_p r_0(x)/k_R$, we take

$$\bar{R}_0 = \frac{\bar{V}_p}{k_R}, \tag{20}$$

so that

$$\bar{v}_p = g_r, \qquad R_0(x) = \bar{R}_0 r_0(x) = \bar{R}_0 \{\rho^2 H(-X) + H(X)\}. \tag{21}$$

We are interested in a time-independent steady state solution $\bar{a}(x, z)$, $\bar{b}(x, z)$, and $\bar{r}(x, z)$ for the system (12)–(16). For such a solution, we may set all time derivatives in these equations to zero to get

$$0 = \nabla^2 \bar{a} - h_z \bar{a}\bar{r} + f_z \bar{b} + v_L(x), \tag{22}$$

and

$$0 = h_z \bar{a}\bar{r} - (f_z + g_z)\bar{b}, \qquad 0 = v_R(x) - h_z \bar{a}\bar{r} - g_r \bar{r} + f_z \bar{b}, \tag{23}$$

for $(x, z) \in \Omega$. The nonlinear system of ODE (22)–(23) is augmented by the boundary conditions (14)–(15). With $v_L(x)$ and $v_R(x)$ both piecewise constant, the form of the (22)–(23) requires that $\bar{a}$ and its first derivative to be continuous at $x = 0$.

3.2. ***Reduction to a single equation for $\bar{a}(x)$.*** The two equations in (23) may be solved for $\bar{b}$ and $\bar{r}$ in terms of $\bar{a}$ to obtain

$$\bar{r} = \frac{\alpha_z r_0(x)}{\alpha_z + \zeta \bar{a}}, \qquad \bar{b} = \frac{r_0(x)\bar{a}}{\alpha_z + \zeta \bar{a}}, \tag{24}$$

where

$$\zeta = \frac{g_z}{g_r} = \frac{k_{\text{deg}}}{k_R}, \qquad \alpha_z = \frac{g_z + f_z}{h_z}\,. \tag{25}$$

The expressions in (24) are now used to eliminate $\bar{r}$ and $\bar{b}$ from (22) to get a second-order PDE for $\bar{a}$ alone:

$$\nabla^2 \bar{a} - \frac{g_z r_0(x)\bar{a}}{\alpha_z + \zeta \bar{a}} + v_L(x) = 0 \qquad (x, z) \in \Omega. \tag{26}$$

Equation (26) is supplemented by the four boundary conditions (14)–(15) applied to $\bar{a}$, keeping in mind also the continuity conditions on the unknown and its normal derivative at $x = 0$.

For our choice of synthesis rates V_L and V_R, we have $v_L = 0$ and $r_0(x) = 1$ for the range $0 < x < \ell_M$ so that

$$\nabla^2 \bar{a} = \frac{g_z \bar{a}}{\alpha_z + \zeta \bar{a}} = \frac{g_r \bar{a}}{\alpha_r + \bar{a}}, \qquad \alpha_r = \frac{g_r}{g_z}\alpha_z \tag{27}$$

for (x, z) in $\Omega_0 = \{0 < x < \ell_M,\ 0 < z < 1\}$. In the complementary range $\Omega_m = \{-x_m < x < 0,\ 0 < z < 1\}$, we have $v_L = \bar{v}_z$ and $r_0(x) = \rho^2$ so that

$$\nabla^2 \bar{a} - \frac{g_z \rho^2 \bar{a}}{\alpha_z + \zeta \bar{a}} + \bar{v}_z = 0, \tag{28}$$

for (x, z) in Ω_m and for some known ρ^2 in the range $0 \le \rho^2 \le 1$.

3.3. ***Existence and uniqueness of steady state behavior.*** The governing PDE (26) for the present extracellular model is similar to the corresponding ODE investigated in [Lander et al. 2005b]. This observation effectively allows us to extend the results for the one-dimensional model there to show existence and uniqueness for the two-dimensional model of this paper.

Proposition 1. *There is a unique set of nonnegative steady state concentration gradients $\bar{a}(x, z)$, $\bar{b}(x, z)$ and $\bar{r}(x, z)$ characterized by the two-point boundary value problem (14), (15), (26) and the continuity conditions on $\bar{a}$ and $\partial\bar{a}/\partial x$ at $x = 0$.*

To prove existence, we observe that $a_\ell(x, z) \equiv 0$ is a *lower solution* of the BVP for $\bar{a}(x, z)$ [Sattinger 1972] since it satisfies the inequality

$$-\nabla^2[a_\ell] + \frac{g_z r_0(x) a_\ell}{\alpha_z + \zeta a_\ell} - v_L(x) = -v_L(x) = -\bar{v}_z H(-x) \le 0, \qquad (x, z) \in \Omega$$

and the four relevant boundary conditions, the latter exactly. Also,

$$a_u(x, z) = \bar{v}_z\left\{(\ell_M - x)x_m + \tfrac{1}{2}(\ell_M^2 - x^2)\right\}$$

with

$$(i) \quad a_u(x) \ge 0, \qquad (ii) \quad \frac{\partial a_u}{\partial x}(x) = -\bar{v}_z(x + x_m) < 0 \qquad (-x_m < x \le \ell_M), \quad .$$

is an *upper solution* [Sattinger 1972]. Note that property (ii) ensures $0 \le a_u(x) \le a_u(-x_m)$ in $[-x_m, \ell_M]$. With $a_u(x) > 0$ for $-x_m \le x < \ell_M$, we have

$$-\nabla^2[a_u] + \frac{g_z r_0(x) a_u}{\alpha_z + \zeta a_u} - v_L(x) = \bar{v}_z + \frac{g_z a_u}{\alpha_z + \zeta a_u} - v_L(x) \ge \frac{g_z a_u}{\alpha_z + \zeta a_u} \ge 0 \qquad (x, z) \in \Omega$$

and

$$\left[\frac{\partial a_u}{\partial x}\right]_{x=-x_m} = 0, \qquad a_u(\ell_M) = 0,$$
$$\left[\frac{\partial a_u}{\partial z} + \gamma_z a_u\right]_{z=1} \ge 0, \qquad \left[\frac{\partial a_u}{\partial z}\right]_{z=0} = 0.$$

There exists then a solution $\bar{a}(x, z)$ of the BVP (26), (14) and (15) with

$$0 = a_\ell(x) \le \bar{a}(x, z) \le a_u(x),$$

for $(x, z) \in \Omega$ (see [Amann 1972], [Sattinger 1972], and [Smoller 1983]). It follows that $\bar{a}(x, z)$ must be nonnegative in the whole solution domain.

To show that there is only one solution, suppose $a_1(x, z)$ and $a_2(x, z)$ are two (nonnegative) solutions and $a(x, z) = a_1(x, z) - a_2(x, z)$. Then as a consequence of the differential equation (26) for a_1 and a_2, the difference $a(x, z)$ satisfies the differential equation

$$-\nabla^2 a + \frac{g_z \zeta \alpha_z r_0(x) a}{(\alpha_z + \zeta a_1)(\alpha_z + \zeta a_2)} = 0.$$

Form the following double integral of the PDE above over the solution domain to get

$$\int_0^1 \int_{-x_m}^{\ell_M} \left[-\nabla^2 a + \frac{g_z \zeta \alpha_z r_0 a}{(\alpha_z + \zeta a_1)(\alpha_z + \zeta a_2)}\right] a \, dx \, dz = 0. \tag{29}$$

Upon integration by parts (by way of Green's theorem), observing continuity of $\bar{a}$ and its first derivatives, and application of the boundary conditions in (14) and (15), the relation (29) may be transformed into

$$\int_{-x_m}^{\ell_M} \left[\frac{a^2}{\sigma_z}\right]_{z=1} dx + \int_0^1 \int_{-x_m}^{\ell_M} \left\{|\vec{\nabla} a|^2 + \frac{g_z \zeta \alpha_z r_0 a^2}{(\alpha_z + \zeta a_1)(\alpha_z + \zeta a_2)}\right\} dx \, dz = 0. \tag{30}$$

All terms in the integrands in (30) are nonnegative; therefore we must have $a(x) \equiv 0$ and uniqueness is proved. □

Note that there is no restriction on the magnitude of the (dimensionless) morphogen production rate $\bar{v}_z$ or the (dimensionless) degradation rate g_z for the existence of steady state concentration gradients. Accordingly, Proposition 1 allows us to obtain exact or approximate solution of the BVP by any choice of analytical or numerical methods.

4. Linear stability

4.1. ***A nonlinear eigenvalue problem.*** In addition to the existence of unique steady state concentrations $\bar{a}(x, z)$, $\bar{b}(x, z)$,and $\bar{r}(x, z)$, it is important for these concentrations to be asymptotically stable (at least

with respect to small perturbations). To investigate the stability of the steady state solution known to exist from Proposition 1, we consider small perturbations in the form

$$\{a, b, r\} = \{\bar{a}(x, z), \bar{b}(x, z), \bar{r}(x, z)\} + e^{-\omega t}\{\hat{a}(x, z), \hat{b}(x, z), \hat{r}(x, z)\}. \tag{31}$$

After linearization, the differential equations (12)–(13) become

$$-\omega\hat{a} = \nabla^2\hat{a} - h_z(\bar{r}\hat{a} + \bar{a}\hat{r}) + f_z\hat{b}, \tag{32}$$

$$-\omega\hat{b} = h_z(\bar{r}\hat{a} + \bar{a}\hat{r}) - (f_z + g_z)\hat{b}, \tag{33}$$

$$-\omega\hat{r} = -h_z(\bar{r}\hat{a} + \bar{a}\hat{r}) - g_r\hat{r} + f_z\hat{b}. \tag{34}$$

The relations (33) and (34) are then solved for $\hat{b}$ and $\hat{r}$ in terms of $\hat{a}$ making use of $\bar{b} = \dfrac{g_r\bar{a}}{g_z(\bar{a} + \alpha_r)}$ to get

$$\hat{r} = \frac{h_z(\omega - g_z)\bar{r}(x, z)\hat{a}}{(g_r - \omega)(f_z + g_z - \omega) + h_z\bar{a}(x, z)(g_z - \omega)}, \tag{35}$$

$$\hat{b} = \frac{h_z(g_r - \omega)\bar{r}(x, z)\hat{a}}{(g_r - \omega)(f_z + g_z - \omega) + h_z\bar{a}(x, z)(g_z - \omega)}. \tag{36}$$

The expressions (36) and (35) are used to eliminate $\hat{b}$ and $\hat{r}$ from (32) to obtain

$$\nabla^2\hat{a} + [\omega - q_r(x; z, \omega)]\,\hat{a} = 0, \tag{37}$$

where

$$q_r(x; z, \omega) = \frac{h_z\bar{r}(x, z)(g_r - \omega)(g_z - \omega)}{(g_r - \omega)(g_z + f_z - \omega) + h_z\bar{a}(x, z)(g_z - \omega)} \tag{38}$$

$$= \frac{1}{1 + \zeta\bar{\beta}_m A}\,\frac{h_z r_0(x)(g_r - \omega)(g_z - \omega)}{(g_r - \omega)(g_z + f_z - \omega) + (g_z + f_z)(g_z - \omega)\bar{\beta}_m A} \tag{39}$$

$$\equiv \frac{1}{1 + \zeta\bar{\beta}_m A(x, z)}\,\frac{N_r(x; z, \omega)}{D_r(x; z, \omega)}, \tag{40}$$

where we have set

$$\bar{a}(x, z) = \alpha_z\bar{\beta}_m A(x, z), \tag{41}$$

with $A(-x_m, 0) = 1$ so that $\bar{a}(-x_m, 0) = \alpha_z\bar{\beta}_m$. Note that $\bar{\beta}_m$ is known to be positive from the solution of the steady state problem of the previous section. Let

$$\bar{\beta}_m = \frac{\beta_m}{\rho^2 - \zeta\beta_m} \qquad \text{or equivalently} \qquad \beta_m = \frac{\rho^2\bar{\beta}_m}{1 + \zeta\bar{\beta}_m}; \tag{42}$$

then $\beta_m = \bar{b}(-x_m, 0)$ is positive.

The PDE (37) is supplemented by the boundary conditions (14)–(15) applied to $\hat{a}(x, z)$. Together, (37), (14) and (15) define an eigenvalue problem with ω as the eigenvalue parameter. Though the PDE for $\hat{a}(x, z)$ is linear, the eigenvalue problem is nonlinear since ω appears nonlinearly in $q_r(x; z, \omega)$ so that the homogeneous boundary value problem defined by (37), (14) and (15) is *not* a Sturm–Liouville problem. Given that $r_0(x)$ (and hence also $\bar{r}(x, z)$ and $\bar{b}(x, z)$) may have at most a simple jump discontinuity at $x = 0$, we expect $\hat{a}$ and $\partial\hat{a}/\partial x$ to be continuous at $x = 0$. In the next subsection, we show that the

eigenvalues of the homogeneous boundary value problem must be positive. The steady state gradients $\bar{a}(x,z)$, $\bar{b}(x,z)$, and $\bar{r}(x,z)$ are therefore asymptotically stable by linear stability theory. Since the proof is based on the same technique as that used for one-dimensional models (see [Lander et al. 2005b] for example), we give it below for the simpler case of uniform receptor synthesis rate which can be easily extended to a discontinuous $v_R(x)$ (leading to a discontinuous $r_0(x)$).

4.2. ***Positive eigenvalues and asymptotic stability.*** For $\rho^2 = 1$, so that $r_0(x) = 1$ for $(x,z) \in \bar{\Omega}$, the various gradient concentrations are continuous across $x = 0$.

Proposition 2. *All the eigenvalues of the nonlinear eigenvalue problem (37), (14) and (15) are real.*

To prove this assertion, suppose ω is a complex eigenvalue and $a_\omega(x)$ an associated nontrivial (generally complex) eigenfunction, then ω^* is also an eigenvalue with eigenfunction $a^*_\omega(x)$, where * denotes complex conjugation. The bilinear relation

$$\int_0^1 \int_{-x_m}^{\ell_M} [a^*_\omega \nabla^2 a_\omega - a_\omega \nabla^2 a^*_\omega]\, dx\, dz = 0$$

(which can be established by integration by parts and applications of the boundary conditions in (14) and (15)) requires

$$\int_0^1 \int_{-x_m}^{\ell_M} \left\{(\omega - \omega^*) - \left[q_r(x;z,\omega) - q_r(x;z,\omega^*)\right]\right\} (a^*_\omega a_\omega)\, dx\, dz = 0. \tag{43}$$

It is straightforward to verify $q_r(x;z,\omega) - q_r(x;z,\omega^*) = -(\omega - \omega^*)\Phi(x;z,\omega\omega^*)$, where

$$\Phi(x,z;\omega\omega^*) = \frac{h_z\{f_z Q(g_p,\omega) + (g_z + f_z)\bar{\beta}_m A(x,z) Q(g_z,\omega)\}}{(1 + \zeta\bar{\beta}_m A) D_r(x;z,\omega) D_r(x;z,\omega^*)},$$

with $D_r(x;z,\omega)$ as defined in (40) and

$$Q(y,\omega) = [y - \mathrm{Re}(\omega)]^2 + [\mathrm{Im}(\omega)]^2 > 0.$$

In that case, the condition (43) becomes

$$(\omega - \omega^*) \int_0^1 \int_{-x_m}^{\ell_M} a_\omega a^*_\omega [1 + \Phi(x;z,\omega\omega^*)]\, dx\, dz = 0. \tag{44}$$

Since the double integral is positive for any nontrivial function $a_\omega(x,z;\omega)$, we must have $\omega - \omega^* = 0$. Hence, ω does not have an imaginary part.

Proposition 3. *All eigenvalues of the nonlinear eigenvalue problem (32)–(34), (14) and (15) are positive and the steady state concentrations $\bar{a}(x,z)$, $\bar{b}(x,z)$ and $\bar{r}(x,z)$ are asymptotically stable by a linear stability analysis.*

If the assertion is false and $\omega \le 0$, let $\hat{a}_\omega(x)$ be a nontrivial eigenfunction of the homogeneous BVP (37), (14) and (15) for the nonpositive eigenvalue $\omega = -|\omega|$. Multiply (37) by $\hat{a}_\omega$ and integrate over the solution domain to get

$$\int_0^1 \int_{-x_m}^{\ell_M} \left\{\hat{a}_\omega \nabla^2 \hat{a}_\omega - q_r(x;z,\omega)(\hat{a}_\omega)^2\right\} dx\, dz = -\omega \int_0^1 \int_{-x_m}^{\ell_M} (\hat{a}_\omega)^2\, dx\, dz.$$

After integration by parts and applications of the homogeneous boundary conditions (14) and (15), we obtain

$$\omega \int_0^1 \int_{-x_m}^{\ell_M} (\hat{a}_\omega)^2 \, dx \, dz = \int_0^1 \int_{-x_m}^{\ell_M} \left| \vec{\nabla} \hat{a}_\omega \right|^2 \, dx \, dz + \int_0^1 \int_{-x_m}^{\ell_M} q_r(x; z, \omega)(\hat{a}_\omega)^2 \, dx \, dz. \tag{45}$$

With $\omega = -|\omega| \leq 0$, we have

$$q_r(x; z, -|\omega|) = \frac{\bar{r}(x, z) h_z (g_z + |\omega|)(g_p + |\omega|)}{(g_r + |\omega|)(g_z + f_z + |\omega|) + h_z \bar{a}(x, z)(g_z + |\omega|)} > 0$$

in Ω. For any nontrivial solution of the eigenvalue problem under the assumption $\omega \leq 0$, the right-hand side of (45) is positive, which contradicts the assumption $\omega = -|\omega| \leq 0$. Hence the eigenvalues of the eigenvalue problem for $\hat{a}$ must be positive and the proposition is proved.

5. Perturbation solution for $\zeta < 1$ and gradient robustness

For Dpp gradients in *Drosophila* wing disc, k_{deg} is typically smaller than the degradation rate constant k_R of the signaling receptor Tkv so that $\zeta < 1$. For this case, a perturbation solution in ζ is appropriate for moderate Dpp synthesis rate resulting in low receptor occupancy (see [Bender and Orszag 1999]):

$$\bar{a}(x, z; \zeta) = \sum_{k=0}^{\infty} \bar{a}_k(x, z) \zeta^k. \tag{46}$$

For sufficiently small values of ζ so that $\zeta \bar{a} \ll \alpha_z$, the leading term $\bar{a}_0(x, z)$, determined by the linear PDE

$$\nabla^2 \bar{a}_0 - \mu_z^2 r_0(x) \bar{a}_0 + v_L(x) = 0, \qquad \mu_z^2 = \frac{g_z}{\alpha_z} \tag{47}$$

and the four boundary condition (14)–(15) applied to $\bar{a}_0$, is an adequate approximation of the exact solution. Here, we have, in terms of the Heaviside unit step function $H(\cdot)$, $r_0(x) = \{H(x) + \rho^2 H(-x)\}$ and $v_L(x) = \bar{v}_z H(-x)$ with $\bar{v}_z = (\bar{V}_L / \bar{R}_0)/(D/Z_{\max}^2)$. The omission of the $\zeta \bar{a}$ term in (26) to get the leading term approximation (47) may also be viewed as a case of *low receptor occupancy* resulting from a sufficiently high receptor synthesis rate (or a sufficiently low morphogen synthesis rate). With plenty of unoccupied receptors available to capture any free Dpp, the normalized morphogen concentration $\bar{a}$ would be sufficiently low for $\zeta \bar{a}$ to be negligible compared to α_z.

The linear BVP (47), (14)–(15) can be solved by Fourier cosine series in the z variable:

$$\{\bar{a}_0(x, z), v_L(x)\} = \sum_{n=1}^{\infty} \{A_n(x), v_n \bar{v}_z H(-x)\} \cos(\lambda_n z) \tag{48}$$

where $\{\lambda_n\}$ are roots of

$$\cot(\lambda) = \sigma_z \lambda, \qquad \sigma_z = \frac{1}{\gamma_z}, \tag{49}$$

so that $\bar{a}_0(x, z)$ satisfies the boundary condition at both $z = 0$ and $z = 1$. Orthogonality of the eigenfunctions $\{\cos(\lambda_n z)\}$ requires

$$v_n = \frac{4 \sin(\lambda_n)}{2\lambda_n + \sin(2\lambda_n)}$$

and

$$A_n'' - \Lambda_n^2 A_n + v_n \bar{v}_z H(-x) = 0, \qquad \Lambda_n^2 = \lambda_n^2 + r_0(x)\mu_z^2, \tag{50}$$

where $\mu_z^2 = g_z/\alpha_z$, with

$$A_n'(-x_m) = 0, \qquad A_n(\ell_M) = 0 \tag{51}$$

for $n = 1, 2, 3, \ldots$. When $\rho^2 = 1$, we expect $A_n(x)$ and $A_n'(x)$ to be continuous at $x = 0$.

Remark 1. The leading term perturbation solution in the small parameter ζ is generally an accurate characterization of the actual nonlinear phenomenon. If $\zeta\bar{a}(x, z)$ should not be small compared to α_z, the gradient [*LR*] for $\rho = 1$ would be nearly uniform in the anteroposterior direction except for a boundary layer near the edge of the wing disc. Such [*LR*] gradients are not biologically realistic for patterning. We may therefore focus our attention on the low receptor occupancy case (with $\zeta\bar{a}(x, z) \ll \alpha_z$) independent of the magnitude of ζ to investigate the effects of size on the signaling morphogen gradient.

To extract useful information from the Fourier cosine series solution (48)–(51), we deduce below a simple but adequate approximation of the leading term perturbation solution, focusing on the special case $\rho(x) = 1$ so that $r_0(x) = 1$ and give special attention to the limiting case of $\ell_M = \infty$.

5.1. ***Finite ℓ_M.*** For special case $\rho(x) = 1$, the exact solution for $A_j(x)$ is

$$A_j(x) = \begin{cases} \dfrac{\bar{v}_z v_j}{\Lambda_j^2}\left(1 - \dfrac{\cosh(\Lambda_j \ell_M)}{\cosh(\Lambda_j(\ell_M + x_m))}\cosh(\Lambda_j(x_M + x))\right) & (-x_m \le x \le 0), \\ \dfrac{\bar{v}_z v_j \sinh(\Lambda_j x_m)}{\Lambda_j^2 \cosh(\Lambda_j(\ell_M + x_m))}\sinh(\Lambda_j(\ell_M - x)) & (0 \le x \le \ell_M). \end{cases} \tag{52}$$

Correspondingly, we have

$$\bar{a}(0, z) \sim \bar{a}_0(0, z) = \bar{v}_z \sum_{j=1}^{\infty} \frac{v_j}{\Lambda_j^2} \frac{\sinh(\Lambda_j x_m)\sinh(\Lambda_j \ell_M)}{\cosh(\Lambda_j(\ell_M + x_m))}\cos(\lambda_j z),$$

$$\bar{a}(-x_m, z) \sim \bar{a}_0(-x_m, z) = \bar{v}_z \sum_{j=1}^{\infty} \frac{v_j}{\Lambda_j^2}\left(1 - \frac{\cosh(\Lambda_j \ell_M)}{\cosh(\Lambda_j(\ell_M + x_m))}\right)\cos(\lambda_j z).$$

With $(v_j/\Lambda_j^2)/(v_1/\Lambda_1^2) \ll 1$ for $j > 1$, we have as a leading term approximation

$$\begin{aligned} b(x, z) &\sim \frac{1}{\alpha_z}\bar{a}(x, z) \sim \frac{1}{\alpha_z}\bar{a}_0(x, z) \approx \frac{1}{\alpha_z} A_1(x)\cos(\lambda_1 z) \\ &= \frac{\bar{v}_z v_1}{\alpha_z \Lambda_1^2} \frac{\sinh(\Lambda_1 x_m)}{\cosh(\Lambda_1(\ell_M + x_m))}\sinh(\Lambda_1(\ell_M - x))\cos(\lambda_1 z). \end{aligned} \tag{53}$$

5.2. ***The limiting case of $\ell_M = \infty$.*** For the wing imaginal disc of *Drosophila* species, $X_{\max} \gg Z_{\max}$ so $\ell_M \gg 1$. It often suffices for our purpose to consider the limiting case of $\ell_M = \infty$ (and $\rho = 1$) for which

$$A_j(x) = \begin{cases} \dfrac{\bar{v}_z v_j}{\Lambda_j^2}\{1 - e^{-\Lambda_j x_m}\cosh(\Lambda_j(x + x_m))\} & (-x_m \le x \le 0), \\ \dfrac{\bar{v}_z v_j}{\Lambda_j^2}\sinh(\Lambda_j x_m) e^{-\Lambda_j(x + x_m)} & (0 \le x < \infty). \end{cases} \tag{54}$$

with

$$\bar{a}(0,z) \sim \bar{a}_0(0,z) = \bar{v}_z \sum_{j=1}^{\infty} \frac{v_j}{\Lambda_j^2} e^{-\Lambda_j x_m} \sinh(\Lambda_j x_m) \cos(\lambda_j z), \tag{55}$$

$$\bar{a}(-x_m,z) \sim \bar{a}_0(-x_m,z) = \bar{v}_z \sum_{j=1}^{\infty} \frac{v_j}{\Lambda_j^2} \left(1 - e^{-\Lambda_j x_m}\right) \cos(\lambda_j z). \tag{56}$$

To a leading term approximation, we have for $\ell_M = \infty$

$$\begin{aligned} b(x,z) &\sim \frac{1}{\alpha_z}\bar{a}(x,z) \sim \frac{1}{\alpha_z}\bar{a}_0(x,z) \approx \frac{1}{\alpha_z} A_1(x)\cos(\lambda_1 z) \\ &= \frac{\bar{v}_z v_1}{\alpha_z \Lambda_1^2} \sinh(\Lambda_1 x_m) e^{-\Lambda_1(x+x_m)} \cos(\lambda_j z) \quad (0 \le x < \infty). \end{aligned} \tag{57}$$

For an [*LR*] gradient to be biologically useful in developing tissue patterns, its graph must be neither nearly uniform nor a boundary layer phenomenon near the source. It follows that the concentration of signaling Dpp–Tkv complexes [*LR*] should be in a state of low receptor occupancy throughout the wing disc with both free and bound Dpp approximately in a state of simple exponential decay from the source end to the sink at the edge of wing disc. With the free Dpp expression exponentially small away from the source, the actual location of the absorbing edge should not have a significant effect on the signaling Dpp gradient and may be taken to be far away at infinity.

6. Approximate expressions for the eigenvalues $\{\lambda_n\}$

6.1. ***A sealed basement membrane*** **($\gamma_z = 0$).** For the limiting case of $\gamma_z = 0$, both apical and basal faces are sealed (see (15)) given that

$$\left[\frac{\partial \bar{a}(x,z)}{\partial z}\right]_{z=1} = \left[\frac{\partial \bar{a}(x,z)}{\partial z}\right]_{z=0} = 0. \tag{58}$$

Upon writing the equation (49) for the eigenvalues as

$$\gamma_z \cos(\lambda) = \lambda \sin(\lambda),$$

we have for $\gamma_z = 0$

$$\lambda_n = (n-1)\pi \qquad (n = 1, 2, \dots). \tag{59}$$

It follows that

$$v_1 = 1, \qquad v_n = 0 \quad (n \ge 2).$$

The concentration gradient is therefore a uniform distribution in z. In that case, the solution for the (normalized) free morphogen concentration $\bar{a}$ is uniform in z so that

$$\bar{a}(x,z) \sim \bar{a}_0(x)\{1 + O(\zeta)\}$$

and $\bar{a}_0(x)$ is just the corresponding solution for the spatially one-dimensional problem previously treated in [Lander et al. 2005b].

For the case $\ell_M = \infty$ (and $\rho = 1$), we have from (57)

$$\frac{[LR(x,z)]}{\bar{R}_0} \sim \frac{\bar{a}_0(x)}{\alpha_z} = \begin{cases} (\bar{v}_z/g_z)\{1 - e^{-\mu_z x_m}\cosh(\mu_z(x+x_m))\} & (-x_m \le x \le 0), \\ (\bar{v}_z/g_z)\sinh(\mu_z x_m)e^{-\mu_z(x+x_m)} & (0 \le x < \infty). \end{cases} \tag{60}$$

with

$$\mu_z^2 = \frac{g_z}{\alpha_z} \simeq h_z, \quad \bar{v}_z = \frac{\bar{V}_L/\bar{R}_0}{D/Z_{\max}^2}, \qquad \frac{\bar{v}_z}{g_z} = \frac{\bar{V}_L/\bar{R}_0}{k_{\deg}}. \tag{61}$$

With $h_z = O(10^{-1})$ for typical wing disc parameter values, we have $\mu_z x_m \ll 1$ and therewith

$$e^{-\mu_z x_m}\sinh(\mu_z x_m) \simeq \mu_z x_m\{1 + O(\mu_z^2 x_m^2)\},$$

so

$$[LR(x,z)] \sim \frac{\bar{R}_0}{\alpha_z}\bar{a}_0(x) \approx \frac{\bar{V}_L}{k_{\deg}}\mu_z x_m e^{-\mu_z x} = \frac{\bar{V}_L X_{\min}}{k_{\deg}}\bar{k}_{\text{on}} e^{-\bar{k}_{\text{on}}X} \tag{62}$$

for the signaling region $0 \le x < \infty$, with $\bar{k}_{\text{on}} = \sqrt{k_{\text{on}}\bar{R}_0/D}$.

We know from biological evidence that the basal end is not sealed, so that the limiting case of $\gamma_z = 0$ only demonstrates the validity and consistency of our more general solution, but is otherwise biologically unrealistic and of no relevance to the actual problem. The analytical consequences of a sealed end, as seen from (62), are shown in the next section to be also unacceptable from the view point of size adjustment for robustness with respect to a substantial change in the Dpp synthesis rate.

6.2. ***An absorbing basement membrane*** **($\sigma_z = 0$).** At the other extreme, Equation (49) in the case of $\sigma_z = 1/\gamma_z = 0$ becomes $\cot(\lambda) = 0$, so that

$$\lambda_n = (n - \tfrac{1}{2})\pi \qquad (n = 1, 2, 3, \dots). \tag{63}$$

It follows that, for the limiting case of $\ell_M = \infty$ and $\rho = 1$,

$$A_j(x) = \begin{cases} (\bar{v}_z v_j/\Lambda_j^2)\{1 - e^{-\Lambda_j x_m}\cosh(\Lambda_j(x+x_m))\} & (-x_m < x < 0), \\ (\bar{v}_z v_j/\Lambda_j^2)\sinh(\Lambda_j x_m)e^{-\Lambda_j(x+x_m)} & (0 < x < \infty). \end{cases} \tag{64}$$

where

$$\Lambda_n^2 = \lambda_n^2 + \mu_z^2 = (n - \tfrac{1}{2})^2\pi^2 + \mu_z^2, \quad v_n = (-)^{n-1}\frac{2}{\lambda_n}, \quad (n = 1, 2, 3, \dots).$$

Correspondingly, we have for the signaling region $0 < x < \infty$

$$\frac{[L]}{R_0} \sim A_1(x)\cos(\lambda_1 z) = \frac{\bar{v}_z v_1}{\Lambda_1^2}\sinh(\Lambda_1 x_m)e^{-\Lambda_1(x+x_m)}\cos(\lambda_1 z), \tag{65}$$

$$\frac{[LR]}{R_0} \sim \frac{A_1(x)}{\alpha_z}\cos(\lambda_1 z) = \frac{\bar{v}_z v_1}{\alpha_z\Lambda_1^2}\sinh(\Lambda_1 x_m)e^{-\Lambda_1(x+x_m)}\cos(\lambda_1 z). \tag{66}$$

With $f_z \ll g_z$, the expression for μ_z^2 is accurately approximated by $h_z = k_{\text{on}}\bar{R}_0/(D/Z_{\max}^2) = O(10^{-1})$. Since μ_z^2 is small compared to $\pi^2/4$ (and much smaller than $(n - \frac{1}{2})^2\pi^2$ for $n \ge 2$) and $\lambda_1 x_m \ll 1$, we have the following accurate approximation for the various Fourier components of the Dpp concentration:

$$\Lambda_n^2 = \lambda_n^2 + \mu_z^2 \simeq \lambda_n^2 = (n - \tfrac{1}{2})^2\pi^2, \qquad \sinh(\lambda_1 x_m)e^{-\lambda_1 x_m} \approx \lambda_1 x_m, \tag{67}$$

$$A_j(x) \simeq \frac{\bar{v}_z v_j}{\lambda_j^2}\sinh(\lambda_j x_m)e^{-\lambda_j(x_m+x)} \qquad (0 < x < \infty) \tag{68}$$

so that

$$[L] \sim \bar{R}_0\bar{a}_0(x,z) \approx \bar{R}_0 A_1(x)\cos(\lambda_1 z) \simeq \frac{\bar{R}_0\bar{v}_z v_1 x_m}{\lambda_1}e^{-\lambda_1 x}\cos(\lambda_1 z), \tag{69}$$

$$[LR] \sim \frac{\bar{R}_0}{\alpha_z}\bar{a}_0(x,z) \simeq \frac{\bar{R}_0\bar{v}_z v_1 x_m}{\alpha_z\lambda_1}e^{-\lambda_1 x}\cos(\lambda_1 z), \tag{70}$$

for $0 < x < \infty$. Upon observing (67) and setting $\Lambda_n^2 \approx \lambda_n^2$, (69) and (70) become

$$[L] \sim \frac{\bar{V}_L X_{\min} Z_{\max}}{D}\left[\frac{8}{\pi^2}e^{-\pi x/2}\cos(\tfrac{1}{2}\pi z)\right], \tag{71}$$

$$[LR] \sim \frac{\bar{V}_L X_{\min} Z_{\max}}{D}\left[\frac{8}{\alpha_z\pi^2}e^{-\pi x/2}\cos(\tfrac{1}{2}\pi z)\right], \tag{72}$$

for $0 < x < \infty$. The signaling Dpp gradient given in (70) and (72) is qualitatively different from that in (62) and (72). While the limiting case of $\sigma_z = 0$ is also not biologically realistic as the basement membrane is neither completely sealed nor absorbing [Dowd et al. 1999], the consequences of (70) are more characteristic of the $[LR]$ gradient than those of (62) in the actual range of γ_z as we shall see in the next subsection.

It may seem rather remarkable that (the leading term asymptotic behavior of) $[LR]$ does not depend on the receptor synthesis rate. However the inherent assumption of low receptor occupancy in effect corresponds to (an abundance of receptors resulting from) a sufficiently high receptor synthesis rate to make its magnitude inconsequential in a first approximation theory.

6.3. ***Eigenvalues for small and large σ_z.*** We now turn to the biologically more realistic case of a leaky basement membrane at $Z = Z_{\max}$ with a finite $\gamma_z = 1/\sigma_z$. For the wing disc problem, we have $0 < \sigma_z < 1$ and a perturbation solution for λ in a power series in σ_z gives

$$\lambda_n = \left(n - \tfrac{1}{2}\right)\pi\left[1 - \sigma_z + O(\sigma_z^2)\right], \tag{73}$$

for $n = 1, 2, 3, \ldots$. No new eigenpairs arise from nonpositive integers n. We conclude (as in the limiting case of an absorbing basal end):

Proposition 4. *For $0 < \sigma_z = 1/\gamma_z < 1$, the expression (70) is an accurate leading term approximation for the signaling Dpp gradient outside the Dpp production region where the $[LR]$ gradient is instrumental for the wing disc development. Thus, with a permeable (leaky) basement membrane with $0 < \sigma_z < 1$, the slope and convexity (but not the magnitude) of the signaling Dpp gradient in both X and Z direction depends only on the parameter σ_z for the biologically realistic case of low receptor occupancy.*

It appears that a leaky basement membrane serves the purpose of regulating the availability of Dpp at a level that maintain the signaling Dpp gradient *shape*. That is, the *slope* and *convexity* of the $[LR]$ concentration gradient are not sensitive to the synthesis rate $\bar{V}_L$ as it changes with significant environmental perturbations. On the other hand, the magnitude of the bound morphogen concentration is seen from (72) to be proportional to $\bar{V}_L$ (as well as the two length quantities $X_{\min}$ and $Z_{\max}$ and inversely

proportional to the diffusion coefficient D and the composite parameter $\alpha_z = (k_{\text{off}} + k_{\text{deg}})/\bar{R}_0 k_{\text{on}}$ of the binding, dissociation and degradation rate constants).

For completeness, consider also the low leakage case of $\sigma_z \gg 1$ or $0 < \gamma_z \ll 1$. For this case, we may seek a singular perturbation solution for λ in γ_z to obtain

$$\lambda_1 \sim \sqrt{\gamma_z}\left[1 - \tfrac{1}{6}\gamma_z + O(\gamma_z^2)\right], \qquad \lambda_{k+1} \sim k\pi\left[1 + \frac{1}{(k\pi)^2}\gamma_z + O(\gamma_z^2)\right] \tag{74}$$

for $k = 1, 2, \ldots$, with no new eigenpair arising from negative square roots and negative k. The results reduce to those of the limiting case of $\gamma_z = 0$ given in (59) with leading term approximation for $[LR(x, z)]$ for $\ell_M = \infty$ and $\rho = 1$ as previously given in (62). For this (biologically unrealistic) low leakage case, the signaling gradient *shape* is much more sensitive to the leakage parameter γ_z and the degradation-to-binding rate ratio (but not the Dpp synthesis rate $\bar{V}_L$) since we have now

$$\Lambda_1^2 = \lambda_1^2 + \mu_z^2 \sim \gamma_z + \mu_z^2.$$

7. Signaling gradient and wing disc size change

The need to accommodate exogenous environmental changes is a major performance objective of morphogen systems. Given a lack of information on the change in system characteristics caused by such changes, we pursue in this and the next section a more limited objective by investigating the change of signaling morphogen gradient in response to a doubling of Dpp synthesis rate (whatever the cause may be) while all system characteristics remain unchanged. We determine here whether a specific aspect of system architecture, namely, the wing disc size, offers the potential of meeting the performance objective by maintaining the $[LR]$ concentration magnitude and its gradient shape (and thereby preserving tissue pattern) relative to the new size. The concept of robustness is quantified in the next section (see also [Lander et al. 2005c; Vargas 2007]) and used to analyze the sensitivity of the signaling Dpp gradient to the morphogen synthesis rate change and how wing disc size changes may ameliorate this sensitivity. In this section, robustness is taken informally to mean no biologically or functionally significant change in the magnitude and shape of the signaling Dpp gradient $[LR]$ under a significant change in Dpp synthesis rate. (More quantitative measures of robustness will be discussed in the next section.)

We begin by focusing on the case $\ell_M = \infty$ and recalling the following four observations from the results of the previous sections:

1. The apical-basal height of wing disc cells of *Drosophila*s is considerably larger than the lineal dimension of its cross section in the plane of the wing disc. Typically, we have of $x_m = X_{\min}/Z_{\max} = O(10^{-1}) \ll 1$ or smaller so that $0 < \lambda_1 x_m \ll 1$, resulting in $\sinh(\lambda_1 x_m)e^{-\lambda_1 x_m} \approx \lambda_1 x_m$.
2. The basal membrane is in reality neither sealed nor completely absorbing; instead there is a significant amount of leakage with $\gamma_z = 1/\sigma_z > 1$. Consequently, the approximate expression (73) for the eigenvalues $\{\lambda_j\}$ and Proposition 4 for the signaling gradient apply.
3. With μ_z^2 accurately given by $h_z = k_{\text{on}}\bar{R}_0/(D/Z_{\max}^2) = O(10^{-1}) \ll 1 < \pi^2/4$ for a wing imaginal disc with a relatively high leakage through the basal membrane, it follows from (67) that

$$\Lambda_1^2 = \lambda_1^2 + \mu_z^2 \simeq \lambda_1^2 = O\left(\frac{\pi^2}{4}\right) \tag{75}$$

for $\gamma_z = 1/\sigma_z > 1$ so that $\lambda_1 x_m \ll 1$ and $\sinh(\Lambda_1 x_m)e^{-\Lambda_1 x_m} \simeq \lambda_1 x_m$.

4. Anticipating the need to reduce wing disc span ($X_{\max}$ and $X_{\min}$) and cell height ($Z_{\max}$) to maintain robustness, we note that the approximation $\Lambda_1^2 \approx \lambda_1^2$ for the relevant range $\gamma_z = 1/\sigma_z > 1$ improves with smaller wing disc size. It follows from the fact that a reduction in $Z_{\max}$ further reduces the effect of μ_z^2 (which was already minimal according to Proposition 4). This allows us to make the same approximation for smaller $Z_{\max}$ (or $X_{\min}$ and $X_{\max}$). For $\tilde{Z}_{\max} = Z_{\max}/\sqrt{2}$, we have

$$\frac{\tilde{\Lambda}_1}{\Lambda_1} = \frac{\sqrt{1+\tilde{\mu}_z^2/\lambda_1^2}}{\sqrt{1+\mu_z^2/\lambda_1^2}} = \frac{\sqrt{1+\mu_z^2/2\lambda_1^2}}{\sqrt{1+\mu_z^2/\lambda_1^2}} \approx 1 - \frac{\mu_z^2}{4\lambda_1^2} \tag{76}$$

so that the approximation $\tilde{\Lambda}_1^2 \approx \Lambda_1^2$ is accurate to within than 4%.

Given that the higher harmonic terms in the eigenfunction expansion for $\bar{a}_0(x,z)$ are negligibly small compared to the leading term, the four observations above lead to the following accurate approximate expression for the signaling gradient

$$[LR] \approx L_{R0}\frac{v_1}{\alpha_z\lambda_1}e^{-\lambda_1 x}\cos(\lambda_1 z), \qquad L_{R0} = \frac{\bar{V}_L X_{\min} Z_{\max}}{D} \tag{77}$$

in the range $0 < x < \infty$ as was found earlier in (70). Averaging $[LR]$ over the interval $[0, Z_{\max}]$ gives

$$[\overline{LR}] \equiv \frac{1}{Z_{\max}}\int_0^{Z_{\max}} [LR]dZ = \int_0^1 [LR]dz \approx L_{R0}\frac{v_1}{\alpha_z\lambda_1}e^{-\lambda_1 x}\frac{\sin(\lambda_1)}{\lambda_1} \tag{78}$$

with $\lambda_1 \approx \pi(1-\sigma_z)/2$ for $0 \le \sigma_z < \frac{1}{2}$.

We now arrive at the key development of this paper. Suppose the *Dpp* synthesis rate is doubled from $\bar{V}_L$ to $\tilde{V}_L = 2\bar{V}_L$. The maximum magnitude of the signal morphogen gradient (which, for the signaling range $[0,\infty)$, occurs at $x = 0$) would then be doubled since the signaling gradient is proportional to $\bar{V}_L$. The factor $(v_1/\alpha_z\lambda_1)e^{-\lambda_1 x}$ in (77) does not depend on $X_{\min}$ and $Z_{\max}$ explicitly, so the magnitude of $[LR]_{z=0}$ (at least the leading term approximation) may be brought back down to the same level prior to the synthesis rate doubling by reducing either $X_{\min}$ or $Z_{\max}$ by half. Either change would lead to a significant distortion of the developed wing disc. There is however the biologically more realistic alternative of reducing both size parameters by a factor of $\sqrt{2}$. Given $\tilde{X}_{\min} = X_{\min}/\sqrt{2}$ and $\tilde{Z}_{\max} = Z_{\max}/\sqrt{2}$ along with observation (4) above, the new signaling gradient with the modified parameters of this option becomes

$$[\widetilde{LR}]_{z=0} \approx \tilde{L}_{R0}\frac{v_1}{\alpha_z\lambda_1}e^{-\lambda_1 x} = L_{R0}\frac{v_1}{\alpha_z\lambda_1}e^{-\lambda_1 x} \qquad (0 < x < \infty), \tag{79}$$

with $\tilde{L}_{R0} = \tilde{V}_L\tilde{X}_{\min}\tilde{Z}_{\max}/D = \bar{V}_L X_{\min} Z_{\max}/D = L_{R0}$. The right-hand side is just the expression for $[LR]_{z=0}$ in (77). Since the signaling gradient $[LR]$ remains a decaying exponential with the same magnitude at the same scaled proximal-distal location, the *size-normalized* signaling gradient is identical to the corresponding gradient prior to morphogen synthesis rate doubling (though the wing disc size has been reduced). We refer to such preservation of signal gradient shape as *size-normalized robustness* in subsequent developments. Note that the apical-basal average of $[LR]$ as given in (78) is clearly also size–normalized robust.

Among the three options for maintaining the signaling gradient shape after Dpp synthesis rate doubling, halving the anteroposterior span (and hence $X_{\min}$ and $X_{\max}$) alone would mean a more drastic reduction

in the wing disc span in the distal-proximal direction. The resulting new wing disc would be skewed in one direction. At the other extreme, halving $Z_{\max}$ alone would change the shape of the gradient for $x > 0$, given that the exponential factor $e^{-\lambda_1 x}$ becomes $e^{-\lambda_1 X/\tilde{Z}_{\max}} = e^{-\lambda_1 (X/Z_{\max})/2}$. Neither is consistent with the often observed consequence of a substantial increase in ambient temperature: a smaller wing disc that is essentially similar to the normal wing imaginal disc in tissue patterning [de Moed et al. 1997; French et al. 1998; Bitner-Mathé and Klaczko 1999; Azevedo et al. 2002]. Hence, we are led to the following proposition (for $\ell_M = \infty$):

Proposition 5. *When there is a significant increase in the Dpp synthesis rate by a factor M with $\tilde{V}_L = M\bar{V}_L$ and the approximation (77) for [LR] holds, the Drosophila wing imaginal disc patterning is preserved by the size reduction $\tilde{X}_{\min} = X_{\min}/\sqrt{M}$ and $\tilde{Z}_{\max} = Z_{\max}/\sqrt{M}$.*

The reduction of $X_{\min}$ and $Z_{\max}$ (as well as $X_{\max}$ in the case of a finite ℓ_M) by the same amplification factor $1/\sqrt{M}$ is known as *self-similar size reduction*. With such a size reduction, the development of the wing disc is insensitive to an M fold increase in Dpp synthesis rate and is therefore *size-normalized robustness*.

It is worth digressing to comment briefly on the biologically unrealistic case $\gamma_z = 0$. Had the basal end been sealed so that (62) applies with

$$[LR(x,z)] \sim \frac{\bar{V}_L X_{\min}}{k_{\deg}} \bar{k}_{\on} e^{-\bar{k}_{\on} X}, \tag{80}$$

the only way to maintain the concentration magnitude $[LR(0,z)]$ by a size change when $\bar{V}_L$ is doubled would be to reduce $X_{\min}$ by half (instead of by $\sqrt{2}$ as in the case of a leaking basal membrane). The size reduction would not be self-similar unless $Z_{\max}$ is also reduced by half. In this latter case, the size reduction would be self-similar size but substantially more drastic than those observed. Thus a porous basement membrane appears to serve an important function in the robust development of the wing disc.

For the case of a large but finite $X_{\max}$, the expression (53) simplifies to

$$\begin{aligned}[LR(x,z)] &\sim \frac{\bar{R}_0}{\alpha_z}\bar{a}(x,z) \sim \frac{\bar{R}_0}{\alpha_z}\bar{a}_0(x,z) \approx \frac{\bar{R}_0}{\alpha_z} A_1(x)\cos(\lambda_1 z) \\ &\simeq L_{R0}\frac{v_1 e^{-\lambda_1 x}}{\alpha_z \lambda_1}\left(1 - e^{-2\lambda_1(\ell_M - x)}\right)\cos(\lambda_1 z),\end{aligned} \tag{81}$$

for $\Lambda_1 x_m \simeq \lambda_1 x_m \ll 1$ (keeping in mind that $L_{R0} = \bar{V}_L X_{\min} Z_{\max}/D$). We have from this the following extension of Proposition 5:

Proposition 6. *For a finite (dimensionless) anteroposterior span ℓ_M, the signaling Dpp gradient is (size-normalized) robust after a Dpp synthesis rate doubling provided that $X_{\max}$ is also reduced by the same factor $\sqrt{2}$ (as $X_{\min}$ and $Z_{\max}$).*

We emphasize that there are at least three advantages in changing both $X_{\min}$ and $Z_{\max}$ (as well as $X_{\max}$) by the same factor to maintain the shape (that is, slope and convexity) of the signaling gradient [*LR*] when the Dpp synthesis rate is doubled:

1. The size of the wing disc is reduced in all dimensions but the physical shape remains geometrically similar before and after the reduction.

2. The reduction is less drastic, by only a factor of $\sqrt{2}$ instead of half.
3. Most importantly, it is consistent with the observation that fly wings are smaller physically in all directions under the higher temperature, not just in the direction of the anteroposterior axis.

8. Robustness of signaling gradients

We saw from the eigenfunction expansion for the leading term perturbation solution that the signaling [*LR*] gradient is generally sensitive to system parameter changes. Yet actual biological systems are generally robust to such changes (up to a self-similar size change [de Moed et al. 1997; French et al. 1998; Bitner-Mathé and Klaczko 1999; Azevedo et al. 2002]). The analysis of the previous section showed that the magnitude and shape of the signaling gradient [*LR*] can be maintained even when the Dpp synthesis rate increases substantially by changing the anteroposterior span (including the width of the localized Dpp synthesis region) and apical-basal cell height of the wing disc. In this section we quantify this observation by way of either of the two robustness indices to be introduced below and generalize the mechanism of self-similar size reduction for more flexible applications. To be concrete, we focus on robustness with respect to a two-fold change in the Dpp synthesis rate in our model problem as in [Lander et al. 2005c]. The general methodology developed for this parameter change is extended to allow for multifactor changes and robustness with respect to other parameter changes in Section 9.

With a doubling of the morphogen synthesis rate $\tilde{V}_L = 2\bar{V}_L$, we have chosen in the previous section an "amplification" (or a "diminution") factor κ (with $\tilde{X}_{\min} = \kappa X_{\min}$, $\tilde{Z}_{\max} = \kappa Z_{\max}$ as well as $\tilde{X}_{\max} = \kappa X_{\max}$) to be $1/\sqrt{M} = 1/\sqrt{2}$ to maintain the order of magnitude of $A_1(0)$. However, the shape of the new signaling gradient is preserved by such a change only after the approximation $\tilde{\Lambda}_n^2 \approx \Lambda_n^2$. For $\gamma_z = 2$ however, the error incurred for the dominant $n = 1$ term in the eigenfunction expansion is about 15%. We explore in this section how we may limit the effects on Λ_1^2 (and more generally Λ_n^2) resulting from more general size changes of $Z_{\max}$ and $X_{\min}$ when $\gamma_z = O(1)$ (but < 2).

For the particular case of Dpp synthesis rate doubling, there is nothing canonical about reducing $Z_{\max}$ and $X_{\min}$ by a factor $\sqrt{2}$ to minimize the change in $[LR(0, z)]$. If we should reduce $Z_{\max}$ (as well as $X_{\min}$ and $X_{\max}$) by a different factor κ instead,

$$\{\tilde{X}_{\min}, \tilde{Z}_{\max}, \tilde{X}_{\max}\} = \kappa \{X_{\min}, Z_{\max}, X_{\max}\}, \tag{82}$$

(e.g., $\kappa = 1/\sqrt{3}$), the new concentration parameter $\tilde{L}_{R0}$ would generally not be the same as L_{R0} as desired, smaller if $\kappa^2 < \frac{1}{2}$ (e.g., $\tilde{L}_{R0} = 2L_{R0}/3$ when $\kappa = 1/\sqrt{3}$) and greater if $\kappa^2 > \frac{1}{2}$. While neither appears ideal for maintaining the magnitude of [*LR*] at $x = 0$ after synthesis rate doubling, the added flexibility may offer alternative benefits for $x > 0$ given that (75) is only an approximate relation and (73) only holds for the biologically realistic range $\sigma_z \ll 1$. This flexibility is explored in the next two subsections. For those developments, it should be noted that the ratio (76) describing the change in the gradient shape factor Λ_1 is modified to become

$$\frac{\tilde{\Lambda}_1}{\Lambda_1} = \frac{\sqrt{1 + \kappa^2 \mu_z^2/\lambda_1^2}}{\sqrt{1 + \mu_z^2/\lambda_1^2}} \approx 1 + (\kappa^2 - 1)\frac{\mu_z^2}{2\lambda_1^2}, \tag{83}$$

which remains nearly 1 for a basal membrane with high leakage. The possibility of specifying κ enables us to choose it to minimize the effect of size changes on two robustness indices that measures the relative change in the magnitude and shape of the signaling [*LR*] gradient downstream.

8.1. ***Root-mean-square differential signaling.*** To quantify the advantage of a smaller κ (than $1/\sqrt{2}$), we let $\bar{b}(x,z)$ and $\tilde{b}(x,z)$ be the normalized signaling morphogen-receptor gradients for morphogen synthesis rate $\bar{V}_L$ and $\tilde{V}_L = 2\bar{V}_L$, respectively. We have, for the low receptor occupancy case,

$$\{\bar{b}(x,z),\ \tilde{b}(x,z)\} \sim \frac{1}{\alpha_z}\{\bar{a}_0(x,z),\ \tilde{a}_0(x,z)\} \approx \frac{\cos(\lambda_1 z)}{\alpha_z}\{A_1(x),\ \tilde{A}_1(x)\}$$

where $A_1(x)$ (for $\rho = 1$ and $\ell_M = \infty$) is as in (54) and $\tilde{A}_1(x,z)$ is $A_1(x)$ with $\bar{v}_z = (\bar{V}_L/\bar{R}_0)/(D/Z_{\max}^2)$ replaced by $\tilde{v}_z = (\tilde{V}_L/\bar{R}_0)/(D/\tilde{Z}_{\max}^2)$, for $\tilde{Z}_{\max} = \kappa Z_{\max}$ (and $\{\tilde{X}_{\min}, \tilde{X}_{\max}\} = \kappa\{X_{\min}, X_{\max}\}$). Consider the following measure of deviation from the signaling Dpp concentration [*LR*], namely, the *signal robustness index* R_b defined by

$$R_b(\kappa) = \frac{(\Delta b)_{\rm rms}}{b_h - b_\ell} = \frac{1}{b_h - b_\ell}\sqrt{\frac{1}{x_\ell - x_h}\int_{x_h}^{x_\ell}[\tilde{b}(x,0) - \bar{b}(x,0)]^2 dx} \tag{84}$$

where $0 < b_\ell = \bar{b}(x_\ell, 0) < b_h = \bar{b}(x_h, 0) \le \bar{b}(0,0)$, with $0 \le x_h < x_\ell \le \ell_M$. It is just the root-mean-square deviation from $\bar{b}(x,0)$, the normalized signaling gradient $[LR]/\bar{R}_0$ along the apical face over a relevant span of the wing disc. The quantities x_ℓ and x_h (or b_ℓ and b_h) may be chosen away from the extremities to minimize the effects of outliers. (A more encompassing measure would be to use the average value of $\tilde{b}(x,z)$ and $\bar{b}(x,z)$ over the interval $0 < z < 1$ instead of their respective value at $z = 0$. However, it suffices to use the simpler expression (84) in a proof of concept discussion.)

With the doubling of the morphogen synthesis rate from $\bar{V}_L$ to $\tilde{V}_L = 2\bar{V}_L$, we reduce both $X_{\min}$ and $Z_{\max}$ (as well as $X_{\max}$) by an amplification factor κ to make $R_b(\kappa)$ as small as possible to minimize the sensitivity of the signaling gradient to the synthesis rate doubling (and size changes). Alternatively, we may choose instead a value for κ so that $R_b(\kappa)$ is in an acceptable range of values, say $R_b(\kappa) < 0.1$, in order for the root mean square deviation to be effectively less than 10% of the gradient prior to the Dpp synthesis rate doubling.

For the low receptor occupancy case, an explicit expression can be obtained for R_b. For $x_h = 0$ and $x_\ell = 2$ (for which $e^{-2\tilde{\Lambda}_1 x_\ell}$ is negligibly small), we have

$$R_b(\kappa) \simeq \frac{1}{\sqrt{10}}\left(\frac{4\kappa^4}{\tilde{\Lambda}_1^3} + \frac{1}{\Lambda_1^3} - \frac{8\kappa^2}{\Lambda_1\tilde{\Lambda}_1(\tilde{\Lambda}_1 + \Lambda_1)}\right)^{1/2}. \tag{85}$$

The minimum value for this R_b expression is attained at

$$\kappa_{\min}^2 = \frac{\xi^2}{1+\xi}, \qquad \xi = \frac{\tilde{\Lambda}_1}{\Lambda_1}. \tag{86}$$

Table 1 on the next page shows some results for $\kappa_{\min}$ and several other values of κ for $x_\ell = 2$, $x_h = 0$ and the typical set of system parameter values used in [Lander et al. 2005c] (with the dimensionless parameter values $g_z = 0.002$, $f_z = 0.00001$, $h_z = 0.1$, $g_r = 0.01$ and $x_m = X_{\min}/Z_{\max} = 0.1$). For the three values of the leakage parameters used, $\sigma_z = 0.2$, 0.5, and 1.0, the corresponding first eigenvalue being $\lambda_1 \simeq 1.31$,

	$\sigma_z = 1/\gamma_z$		
$1/\kappa^2$	1.0	0.5	0.2
1	0.5223	0.4720	0.4301
2	0.0258	0.0153	0.0095
2.025	0.0198	0.0099	0.0048
2.05	0.0144	0.0057	0.0034
2.10	0.0084	0.0094	0.0119
2.15	0.0147	0.0191	0.0213
3	0.1522	0.1444	0.1354

Table 1. Values of R_b.

1.08, and 0.86, respectively. These results are calculated from the leading term approximation of the eigenfunction expansion for [*LR*] obtained in a previous subsection. Their accuracy has been confirmed by numerical simulations of the nonlinear IBVP in [Vargas 2007].

If the organism size remains unchanged ($\kappa = 1$), the signal robustness index well into the unacceptable range as specified in [Lander et al. 2005c]. A reduction factor of $\kappa = 1/\sqrt{2}$ reduces R_b by a factor greater than 20 to well below the acceptable range of 10%. A slightly smaller κ would reduce R_b toward the minimum point but not practical. Beyond $\kappa_{\min}$ given in (86), further reduction would only worsen the robustness index (and hence the gradient differential).

8.2. ***Root-mean-square signal displacement.*** The signal robustness index R_b is not the only measure of the deviation of the modified signaling gradient from the original one prior to Dpp synthesis rate doubling. Given an existing genetic program for individual cells, a more relevant measure of robustness may be the displacement of the same level of morphogen-receptor complex concentration due to a change of morphogen synthesis rate. Let $\bar{b}(x, 0)$ and $\tilde{b}(x, 0)$ again be the normalized signaling morphogen-receptor gradients at location x on the apical cell surface, $z = 0$, for morphogen synthesis rate $\bar{V}_L$ and $\tilde{V}_L = 2\bar{V}_L$, respectively. Let x and $\tilde{x}$ be the corresponding location where they attain the value b, i.e., $\bar{b}(x, 0) = \tilde{b}(\tilde{x}, 0) = b$. With a change of ligand synthesis rate, $\tilde{x}$ is generally different from x with $\tilde{x} - x = \Delta x$. The root-mean-square of Δx over the range of b would be another meaningful measure of robustness:

$$R_x = \frac{(\Delta x)_{\text{rms}}}{x_\ell - x_u} = \frac{1}{x_\ell - x_u}\sqrt{\frac{1}{b_u - b_\ell}\int_{b_\ell}^{b_u} (\Delta x)^2 db}. \tag{87}$$

To minimize the effects of outliers, we may limit the range of b to be the interval (b_ℓ, b_u) with $0 \le b_\ell < b_u \le \bar{b}(0)$. (We may take $b_\ell = \frac{1}{10}\bar{b}(0)$ and $b_u = \frac{9}{10}\bar{b}(0)$, for instance.)

In general, the dependence of displacement Δx on κ is through the expression

$$\bar{b}(x, 0) \sim \frac{1}{\alpha_z} A_1(x) \approx \frac{\bar{v}_z x_m v_1}{\alpha_z \Lambda_1} \exp(-\Lambda_1 x)$$

for $x \ge 0$ and the corresponding expression for $\tilde{b}(x, 0)$. Inverting these relations, we obtain

$$x \approx -\frac{1}{\Lambda_1} \ln(\eta \Lambda_1 b), \quad \tilde{x} \approx -\frac{1}{\tilde{\Lambda}_1} \ln(\tilde{\eta} \tilde{\Lambda}_1 b), \tag{88}$$

where

$$\eta = \frac{\alpha_z}{\bar{v}_z x_m v_1} = \frac{1}{\beta_z x_m v_1 \mu_z^2}, \qquad \tilde{\eta} = \frac{\eta}{2\kappa^2}, \qquad \beta_z = \frac{\bar{v}_z}{g_z}. \tag{89}$$

From these we obtain

$$\Delta x = \frac{1}{\Lambda_1}\ln(\eta\Lambda_1 b) - \frac{1}{\tilde{\Lambda}_1}\ln(\tilde{\eta}\tilde{\Lambda}_1 b) \equiv c_0(\Lambda_1, \tilde{\Lambda}_1) + c_1(\Lambda_1, \tilde{\Lambda}_1)\ln b, \tag{90}$$

with

$$c_0(\Lambda_1, \tilde{\Lambda}_1) = \frac{1}{\Lambda_1}\ln(\Lambda_1\eta) - \frac{1}{\tilde{\Lambda}_1}\ln(\tilde{\Lambda}_1\tilde{\eta}), \qquad c_1(\Lambda_1, \tilde{\Lambda}_1) = \left(\frac{1}{\Lambda_1} - \frac{1}{\tilde{\Lambda}_1}\right). \tag{91}$$

It follows that

$$R_x = \frac{(\Delta x)_{\text{rms}}}{x_\ell - x_u} = \frac{1}{x_\ell - x_u}\sqrt{\frac{1}{b_u - b_\ell}\int_{b_\ell}^{b_u}\left[c_0(\Lambda_1, \tilde{\Lambda}_1) + c_1(\Lambda_1, \tilde{\Lambda}_1)\ln b\right]^2 db}$$

$$= \frac{1}{x_\ell - x_u}\sqrt{\frac{1}{b_u - b_\ell}\left[c_0^2 b + 2c_0c_1 b(\ln b - 1) + c_1^2\left(b(\ln b)^2 - 2b(\ln b - 1)\right)\right]_{b_\ell}^{b_u}}$$

For sample calculations, we take $b_u = b(0)$ and $b_\ell = b(5) \approx 0$, so that

$$R_x = \tfrac{1}{5}\sqrt{c_0^2 + 2c_0c_1(\ln b_u - 1) + c_1^2\left((\ln b_u)^2 - 2(\ln b_u - 1)\right)} \tag{92}$$

Evidently, R_x should be as small as possible to minimize the deviation from the normal gradient with $R_x = 0$ being no change. Alternatively, we may choose κ so that $R_x(\kappa)$ is in an acceptable range of values. Below are some results for $R_x(\kappa)$ for several choice values of κ for the same typical set system parameter values used for Table 1. However, unlike R_b, the parameter $\bar{v}_z$ now appears explicitly (through η in c_0, see (92), (89) and (91); it was taken so that $\beta_z = \bar{v}_z/g_z = \frac{1}{4}$ for the results in Table 2. These results are calculated from the leading term approximation of the eigenfunction expansion for [*LR*] obtained in a previous subsection. Again, their accuracy has been confirmed by numerical simulations [Strikwerda 1989] of the nonlinear IBVP in [Vargas 2007].

If the organism size remains unchanged, the value of the signal robustness index is well above the acceptable range (see also [Lander et al. 2005c]). An amplification factor $\kappa = 1/\sqrt{2}$ reduces R_x by at least an order of magnitude to well within the acceptable range for (size-normalized) robustness. Beyond the

	$\sigma_z = 1/\gamma_z$		
$1/\kappa^2$	1.0	0.5	0.2
1	0.7564	0.6177	0.5130
1/2	0.0761	0.0407	0.0231
1/2.025	0.0649	0.0316	0.0156
1/2.05	0.0546	0.0239	0.0109
1/2.10	0.0392	0.0200	0.0185
1/2.15	0.0373	0.0331	0.0340
1/2.16	0.0388	0.0365	0.0373
1/3	0.3713	0.3229	0.2783

Table 2. Values of R_x.

	exact		linear	
$1/\kappa^2$	R_b	R_x	R_b	R_x
1	0.3833	0.2488	0.3873	0.2460
2	0.1477	0.1570	0.1422	0.1652
2.75	0.0627	–	0.0543	–
3	0.0503	0.1017	0.0467	0.939
3.75	–	0.0687	–	0.0757
4	0.0661	0.0736	0.0701	0.1206

Table 3. Comparison of exact and approximate values of R_b and R_x (linear approximation).

minimum point (slightly smaller than $1/\sqrt{2}$), a further reduction in κ does not improve R_x but worsens it instead.

8.3. ***General receptor occupancy.*** The analysis and numerical results presented in the previous subsections are based on the leading term perturbation solution for the steady state problem though confirmed by numerical simulation of the corresponding nonlinear IBVP for the low receptor occupancy case. Without the assumption of low receptor occupancy, numerical simulations for the nonlinear BVP (14), (15), and (26) have been carried out in [Vargas 2007] to show that

- size–normalized robustness persists for typical sets of biologically realistic system parameter values, and
- linearized theory is adequate in estimating appropriate self-similar size reduction for size-normalized robustness for the same sets of system parameter values.

Some sample results are shown in Table 3 for $\bar{v}_z = 10^{-3}$ and $\ell_M = 5$ with the remaining parameter values identical to those used for Tables 1 and 2.

9. Multifactor robustness

An exogenous change affects more than just one intrinsic characteristic of a biological organism. While we do not have experimental data to document the effects of a temperature change on other system parameters beside the Dpp synthesis rate, we generally expect the rate constants k_{deg}, k_{off}, k_g and $\bar{V}_R$ to increase with temperature, but are less certain about the effect on the remaining system parameters such as D and k_{on}. We examine here how simultaneous (hypothetical) changes in several system parameters (in response to an external change) may alter the wing disc gradient, at least as dictated by our model. For simplicity, we assume the effect of the external change on the diffusion coefficient D to be negligible in the range of the change considered. Typically, we proceed with the analytical results for the biologically realistic case of low receptor occupancy which enable us to explore how size changes may ameliorate the net effects of the changes in several system characteristics on the signaling gradient. Such an investigation constitutes a first attempt to address theoretically the *multifactor robustness* of temperature change beyond its effects through the single parameter of Dpp synthesis rate.

Some observations can be made immediately about the effect of changing two of the system parameters. First, the dissociation rate constant k_{off} is known to be much smaller than k_{deg} so that $\alpha_z = (g_z + f_z)/h_z \simeq g_z/h_z$. The following is an immediate consequence of this observation and (26):

Proposition 7. *Changes in the dissociation rate constant k_{off} have negligible effect on the signaling Dpp gradient* $[LR]$.

This conclusion is not restricted to the low receptor saturation case, since (26) holds in general.

Next, with $\mu_z^2 = g_z h_z/(g_z + f_z) \simeq h_z = O(10^{-1})$, the approximate expression (67) applies as long as the change in h_z is not larger by an order of magnitude. In that case, Proposition 4 continues to hold and, upon rewriting (70) as

$$[LR] \sim \frac{\bar{V}_L X_{\min} Z_{\max}}{D(k_{\text{deg}} + k_{\text{off}})/k_{\text{on}} \bar{R}_0} \frac{v_1}{\lambda_1} e^{-\lambda_1 x} \cos(\lambda_1 z) \simeq \frac{\bar{V}_L}{k_{\text{deg}}} \frac{\bar{V}_R}{k_g} \frac{k_{\text{on}}}{D/(X_{\min} Z_{\max})} \frac{v_1}{\lambda_1} e^{-\lambda_1 x} \cos(\lambda_1 z) \tag{93}$$

for $0 < x < \infty$, which shows the magnitude of $[LR]$ to increase with the binding rate constant k_{on}, we have the following observation:

Proposition 8. *A substantial change in the binding rate* (*such as doubling its magnitude*) *would have an effect only on the magnitude of the signaling* $[LR]$ *gradient.*

With many rate constants playing a substantive role in the magnitude of the signaling Dpp gradient $[LR]$, many scenarios are possible depending on relative effects of a particular kind of exogenous perturbation (such as a temperature change) on these constants, resulting in the new rate constants $\tilde{V}_L$, $\tilde{V}_R$, $\tilde{k}_{\text{deg}}$, $\tilde{k}_g$, etc., with $m_L = \tilde{V}_L/V_L$, $m_{\text{deg}} = \tilde{k}_{\text{deg}}/k_{\text{deg}}$, and so on. An attempt will be made below to identify some reasonable scenarios and their consequences.

One possible scenario involves the degradation rate constants k_{deg} and k_g changing at the same rate as the corresponding protein synthesis rate $\bar{V}_L$ and $\bar{V}_R$, respectively. In that case, the following is an immediate consequence of (93), with the diffusion rate constant D assumed to be unaffected by the exogenous change:

Proposition 9. *For the low receptor occupancy case, if*

$$\frac{m_L}{m_{\text{deg}}} \equiv \frac{\tilde{V}_L/\bar{V}_L}{\tilde{k}_{\text{deg}}/k_{\text{deg}}} = 1, \qquad \frac{m_R}{m_g} \equiv \frac{\tilde{V}_R/\bar{V}_R}{\tilde{k}_g/k_g} = 1,$$

then a size-normalized robust gradient is attained by a self-similar reduction (*of all spatial lengths*, $X_{\min}$, $Z_{\max}$ *and* $X_{\max}$) *by a factor of* $\sqrt{2}$ *when the binding rate doubles* (*in response to a substantial exogenous change*).

More generally, when $m_L \neq m_{\text{deg}}$ and $m_R \neq m_g$, the situation is more complicated. Upon making use of (93) to form the ratio

$$\frac{[\widetilde{LR}]}{[LR]} \simeq \frac{m_L}{m_{\text{deg}}} \frac{m_R}{m_g} \frac{m_{\text{on}}}{\kappa^2} \tag{94}$$

where $m_{\text{on}} = \tilde{k}_{\text{on}}/k_{\text{on}}$ and where all wing dimensions are changed by the same factor κ so that $\tilde{X}_{\min} = \kappa X_{\min}$, etc., the next proposition also follows from (93):

Proposition 10. *With* $m_D = \tilde{D}/D = 1$, *size-normalized robustness is attained by changing all wing disc dimension by*

$$\kappa^2 = m_{\text{on}} \frac{m_L}{m_{\text{deg}}} \frac{m_R}{m_g}. \tag{95}$$

Evidently, a more optimal κ can be found with the help of the robustness indices R_b and R_x as was done in a previous section on the change for the rate constant $\bar{V}_L$ alone. While the observations in the last two propositions are based on the analytical results, numerical simulations show that they continue to hold for the general model for typical sets of realistic system parameter values.

10. Patterning of a smaller wing disc

It is of some interest to determine also how a higher Dpp synthesis rate and a self-similar size-reduction of the wing imaginal disc may affect the elapsed time to a steady state gradient. Note that the lowest eigenvalue, $\omega^{(0)}$, of the nonlinear eigenvalue problem (37)–(41) provides a good first estimate of this half-life measure. An asymptotic solution for this lowest eigenvalue can be obtained by a regular perturbation solution for $\omega^{(0)}$ in powers of the parameter $\zeta = g_z/g_r < 1$,

$$\omega^{(0)} = \omega_0 + \zeta\omega_1 + \zeta^2\omega_2 + \cdots .$$

Consistent with the low receptor occupancy assumption of this paper (and similar to the development in [Lander et al. 2005b] for the one-dimensional model), the leading term ω_0 is determined by the simpler eigenvalue problem

$$\nabla^2 a_0 + [\omega_0 - q_0(x; z, \omega_0)]\, a_0 = 0, \tag{96}$$

where

$$q_0(x; z, \omega_0) = \frac{h_z r_0(x, z)(g_z - \omega_0)}{g_z + f_z - \omega_0}, \qquad r_0(x, z) = \rho^2 H(-x) + H(x), \tag{97}$$

with the four boundary conditions (14)–(15) applied to $a_0(x, z; \omega_0)$.

To solve this simpler eigenvalue problem, we note that $q_0(x; z, \omega_0)$ is independent of z given that the receptor synthesis rate is chosen so that r_0 depends only on x. We can then separate out the z-dependent part by setting

$$a_0(x, z) = \sum_{j=1}^{\infty} A_j(x) \cos(\lambda_j z),$$

where $\{\lambda_j\}$ are the solutions of (49). Orthogonality of the functions $\{\cos(\lambda_j z)\}$ leads to the eigenvalue problem

$$A_j'' + \big(\omega_0 - \lambda_j^2 - q_0(x; \omega_0)\big) A_j = 0, \qquad A_j'(-x_m) = 0, \qquad A_j(\ell_M) = 0, \tag{98}$$

where a prime $'$ indicates differentiation with respect to x and $j = 1, 2, 3, \ldots$. For $\rho^2 = 1$ so that $r_0(x, z) = 1$ for all $(x, z) \in \bar{\Omega}$, the solutions of the eigenvalue problem (98) are the eigenpairs

$$A_{kj}(x) = a_{kj} \cos(\pi_k(x + x_m)), \qquad \pi_k = \frac{\pi(2k - 1)}{2(\ell_M + x_m)} \tag{99}$$

for $k, j = 1, 2, \ldots$, with

$$\omega_0 = \pi_k^2 + \lambda_j^2 + \frac{h_z(g_z - \omega_0)}{g_z + f_z - \omega_0}. \tag{100}$$

The relation (100) is a quadratic equation for ω_0; finding its two roots, denoted by $\omega_{kj}^{(1)}$ and $\omega_{kj}^{(2)}$, is straightforward. Given $f_z \ll g_z \ll h_z < 1$, these roots are approximated by

$$\omega_{kj}^{(1)} \approx \xi_{kj} \approx \pi_k^2 + \lambda_j^2 + h_z, \qquad \omega_{kj}^{(2)} \approx \frac{\delta_{kj}}{\xi_{kj}} \approx g_z. \tag{101}$$

with $g_z \approx \omega_{kj}^{(2)} \ll \omega_{kj}^{(1)} \approx \pi_k^2 + \lambda_j^2 + h_z$. The decay rate is dominated by the smallest (lowest) $\omega_{kj}^{(2)}$, namely $\omega_{kj}^{(2)} \approx \omega_{11}^{(2)} \approx g_z$. With

$$\omega_{kj}^{(2)} t \approx g_z t = k_{\deg} T,$$

the expression $e^{-g_z t} = e^{-k_{\deg} T}$ gives a half life of $1/k_{\deg}$ which does not vary with size changes in $Z_{\max}$, $X_{\min}$ or $X_{\max}$. We have then the following result on time to steady state gradient:

Proposition 11. *Starting with some small initial* (*perturbation from the steady*) *state*, *the time to a time-independent steady state is determined by the lowest member of the second family of frequencies*, *which is approximately* g_z. *Moreover*, *the corresponding actual half-life is independent of size changes and depends only on* $k_{\deg}$.

It follows that the half life of transients would vary only with a change in $k_{\deg}$ (caused by some exogenous change) and a size change (self-similar or not) would have no effects on this change. In particular, doubling the magnitude of $k_{\deg}$ (caused by a temperature rise) would reduce by half the half life of transients independent of any size changes.

We note that the situation is not the same for the other family $\{\omega_{kj}^{(1)}\}$. With

$$\omega_{kj}^{(1)} \approx \tilde{\omega}_{kj}^{(1)} \equiv \pi_k^2 + \lambda_j^2$$

(which is also independent of the size parameters $\{Z_{\max}, X_{\min}, X_{\max}\}$) and with $t = DT/Z_{\max}^2$, a size change via $Z_{\max}$ by an amplification factor κ leads to

$$T = \frac{t}{D}\tilde{Z}_{\max}^2, \qquad \omega_{kj}^{(1)} t = \frac{D\omega_{kj}^{(1)}}{\tilde{Z}_{\max}^2} T = \frac{D}{\kappa^2 Z_{\max}^2} T(\pi_k^2 + \lambda_j^2). \tag{102}$$

Hence, it would take less time for all harmonics of a smaller disc associated with the first family of (faster) decay rates $\omega_{kj}^{(1)}$ to reach the same level of concentration of $[LR]$. As previously mentioned, size changes have no effect on the actual time to steady state given (102). The main purpose in discussing the family $\{\omega_{kj}^{(1)}\}$ at all is to show that its effect on half life is in the same direction as that of $\omega_{kj}^{(2)} \simeq g_z$ and hence preserving the size-normalized robust nature of the latter when there is a significant exogenous change.

While a reduction of half life of transients is not synonymous with the speed of growth observed in nature, e.g., faster growth of fruit flies in hotter temperature [de Moed et al. 1997; French et al. 1998; Bitner-Mathé and Klaczko 1999; Azevedo et al. 2002], it certainly is not inconsistent with such observations and may very well contribute to its realization.

11. Concluding remarks

Exogenous (environmental) changes, such as a substantial change in ambient temperature, are expected to affect multiple intrinsic system characteristics such as morphogen and receptor synthesis rates, various

binding, dissociation and degradation rate constants, and diffusion rates, of a biological organism. If the effects are substantial as in the case of a 6°C change in ambient temperature on the Dpp synthesis rate in the *Drosophila* wing imaginal disc, they could alter the biological development of the organism. The temperature–Dpp synthesis rate relation, being the only known data of this type, prompted us to initiate an investigation, of at first limited scope, on the effects of exogenous changes on biological development by examining the effect of the synthesis rate change on the signaling Dpp–Tkv concentration gradient. For biologically realistic gradients occurring in the low receptor occupancy range, we show that a signaling gradient is approximately proportional to the Dpp synthesis rate. It is then shown that the effect of a synthesis rate change may be ameliorated by self-similar size changes to result in a (size-normalized) robust development as measured by several different robustness indices introduced in Section 8.

To the extent that a single exogenous perturbation affects generally more than a single system characteristic, the paper also investigates briefly, in the absence of experimental data, how the effects of multiple system characteristic changes on the signaling gradient can also be ameliorated by self-similar size changes, resulting again in size-normalized robustness.

Changes in morphogen gradient shape with temperature and changes in wing disc size with temperature are probably not independent phenomena, given that Dpp and its receptor Tkv control not just cell identity, but also proliferation [Martin et al. 2004; Martin-Castellanos and Edgar 2002]. Indeed, we do not know whether the primary effect of temperature is to change the size of a morphogen field, and then the morphogen gradient responds by re-scaling to fit the new size, or if the primary effect of temperature is on the morphogen gradient, and the patterned field changes its size in response to the morphogen gradient. Most likely reality lies somewhere between these extremes. (We do know, however, that the wing disc BMP gradient can re-scale to fit alterations in disc size imposed by perturbations other than temperature [Teleman and Cohen 2000].)

Clearly, there is much we do not know about the effects of temperature on biological development or, more fundamentally, its interaction with morphogen gradients. Given how important temperature effects are likely to have been in evolution, there is a great need to gather some of the basic information that will be required to understand these effects. The effort of this paper is a step in this direction. Our results have shown that, whether synthesis rate change is a direct or downstream effect of a temperature change, a (self-similar) change of wing disc size would nearly offset the effects of a doubling of morphogen synthesis rate on the signaling gradient to orchestrate a size-normalized development of wing discs.

At the organismic level, flies grow slower at low temperature and to larger size including having larger wings; they have smaller wings and grow faster (but smaller) at higher temperatures [de Moed et al. 1997; French et al. 1998; Bitner-Mathé and Klaczko 1999; Azevedo et al. 2002]. The faster growth rate of the flies at higher temperature is probably related to faster biochemical reactions not addressed by the mathematical model of the present investigation. While the molecular mechanisms that lead to a speed up of the relevant biochemical reactions are unknown to the authors, faster growth may simply be a consequence of (self-similar) size reduction (to maintain size-normalized development robustness) requiring less biological constituent parts for a smaller fly. Time to a steady-state signaling gradient is not synonymous with biological growth rate. Nevertheless, it seems reasonable that the half life to steady state signaling gradient should be consistent with the different growth rate. Given the result of the previous section, it would appear that degradation rate constants k_{deg} should also change

with exogenous temperature perturbations in order to affect the time to a steady state signaling Dpp–Tkv complex gradient (which should contribute to but is unlikely to be completely responsible for the speed of general development and growth). As there are no measurements available to validate the size-normalized multifactor robustness of development (and growth) predicted by our analysis and numerical simulations, it is hoped that observations made herein would stimulate experimental work for measuring the effects of a significant change in temperature on the various rate constants as was done for the Dpp synthesis rate $\bar{V}_L$ (in the Lander lab) mentioned in the first section of this paper.

References

[Amann 1972] H. Amann, "On the existence of positive solutions of nonlinear elliptic boundary value problems", *Indiana Univ. Math. J.* **21**:2 (1972), 125–146.

[Azevedo et al. 2002] R. B. R. Azevedo, V. French, and L. Partridge, "Temperature modulates epidermal cell size in *Drosophila melanogaster*", *J. Insect. Physiol.* **48**:2 (2002), 231–237.

[Bender and Orszag 1999] C. M. Bender and S. A. Orszag, *Advanced mathematical methods for scientists and engineers, I: Asymptotic methods and perturbation theory*, Springer, New York, 1999.

[Bitner-Mathé and Klaczko 1999] B. C. Bitner-Mathé and L. B. Klaczko, "Plasticity of *Drosophila melanogaster* wing morphology: effects of sex, temperature and density", *Genet.* **105**:2 (1999), 203–210.

[Dowd et al. 1999] C. J. Dowd, C. L. Cooney, and M. A. Nugent, "Heparan sulfate mediates bFGF transport through basement membrane by diffusion with rapid reversible binding", *J. Biol. Chem.* **274**:8 (1999), 5236–5244.

[Entchev et al. 2000] E. V. Entchev, A. Schwabedissen, and M. González-Gaitán, "Gradient formation of the TGF-β homolog Dpp", *Cell* **103**:6 (2000), 981–991.

[French et al. 1998] V. French, M. Feast, and L. Partridge, "Body size and cell size in *Drosophila*: the developmental response to temperature", *J. Insect. Physiol.* **44**:11 (1998), 1081–1089.

[Gurdon and Bourillot 2001] J. B. Gurdon and P.-Y. Bourillot, "Morphogen gradient interpretation", *Nature* **413**:6858 (2001), 797–803.

[Khong and Wan 2007] M. Khong and F. Y. M. Wan, "Negative feedback in morphogen gradients", pp. 29–51 in *Frontiers of applied mathematics* (Proc. of 2nd International Symposium) (Beijing, 2006), edited by D.-Y. Hsieh et al., World Scientific, Singapore, 2007.

[Lander et al. 2002] A. D. Lander, Q. Nie, and F. Y. M. Wan, "Do morphogen gradients arise by diffusion?", *Dev. Cell* **2**:6 (2002), 785–796.

[Lander et al. 2005a] A. D. Lander, Q. Nie, B. Vargas, and F. Y. M. Wan, "Aggregation of a distributed source in morphogen gradient formation", *Stud. Appl. Math.* **114**:4 (2005), 343–374.

[Lander et al. 2005b] A. D. Lander, Q. Nie, and F. Y. M. Wan, "Spatially distributed morphogen production and morphogen gradient formation", *Math. Biosci. Eng.* **2**:2 (2005), 239–262.

[Lander et al. 2005c] A. D. Lander, F. Y. M. Wan, and Q. Nie, "Multiple paths to morphogen gradient robustness", preprint, Center for Complex Biological Systems, University of California, Irvine, CA, 2005, available at https://eee.uci.edu/11s/45869/home/Draft5.pdf.

[Lander et al. 2006] A. D. Lander, Q. Nie, and F. Y. M. Wan, "Internalization and end flux in morphogen gradient formation", *J. Comput. Appl. Math.* **190**:1-2 (2006), 232–251.

[Lou et al. 2004] Y. Lou, Q. Nie, and F. Y. M. Wan, "Nonlinear eigenvalue problems in the stability analysis of morphogen gradients", *Stud. Appl. Math.* **113**:2 (2004), 183–215.

[Martin-Castellanos and Edgar 2002] C. Martin-Castellanos and B. A. Edgar, "A characterization of the effects of Dpp signaling on cell growth and proliferation in the *Drosophila* wing", *Dev.* **129**:4 (2002), 1003–1013.

[Martin et al. 2004] F. A. Martin, A. Pérez-Garijo, E. Moreno, and G. Morata, "The *brinker* gradient controls wing growth in *Drosophila*", *Dev.* **131**:20 (2004), 4921–4930.

[de Moed et al. 1997] G. H. de Moed, G. de Jong, and W. Scharloo, "Environmental effects on body size variation in *Drosophila melanogaster* and its cellular basis", *Genet. Res.* **70**:1 (1997), 35–43.

[Sattinger 1972] D. H. Sattinger, "Monotone methods in nonlinear elliptic and parabolic boundary value problems", *Indiana Univ. Math. J.* **21**:11 (1972), 979–1000.

[Smoller 1983] J. Smoller, *Shock waves and reaction-diffusion equations*, Grundlehren der Mathematischen Wissenschaften **258**, Springer, New York, 1983. 2nd ed. published in 1994.

[Strikwerda 1989] J. C. Strikwerda, *Finite difference schemes and partial differential equations*, Wadsworth & Brooks/Cole, Pacific Grove, CA, 1989.

[Teleman and Cohen 2000] A. A. Teleman and S. M. Cohen, "Dpp gradient formation in the *Drosophila* wing imaginal disc", *Cell* **103**:6 (2000), 971–980.

[Umulis et al. 2008] D. M. Umulis, M. B. O'Connor, and H. G. Othmer, "Robustness of embryonic spatial patterning in *Drosophila melanogaster*", *Curr. Top. in Dev. Biol.* **81** (2008), 65–111.

[Vargas 2007] B. Vargas, *Leaky boundaries and morphogen gradient formation*, Ph.D. thesis, University of California, Irvine, CA, 2007.

Received 16 May 2010. Revised 4 Oct 2010. Accepted 6 Oct 2010.

ARTHUR D. LANDER: adlander@uci.edu
Department of Developmental and Cell Biology, University of California, Irvine, 2638 Biological Science III, Irvine, CA 92697-2300, United States
http://lander-office.bio.uci.edu/

QING NIE: qnie@uci.edu
Department of Mathematics, University of California, Irvine, 510B Rowland Hall, Irvine, CA 92697-3875, United States
http://www.math.uci.edu/~qnie/

BENJAMIN VARGAS: paryvargas@hotmail.com
Department of Mathematics, Irvine Valle College, 5500 Irvine Center Drive, Irvine, CA 92618-0300, United States
and
Department of Mathematics, University of California, Irvine, 510B Rowland Hall, Irvine, CA 92697-3875, United States

FREDERIC Y. M. WAN: fwan@uci.edu
Department of Mathematics, University of California, Irvine, 510B Rowland Hall, Irvine, CA 92697-3875, United States
http://www.math.uci.edu/~fwan/